Russian Chemical Reviews **82** (3) 248 – 272 (2013) © 2013 Russian Academy of Sciences and Turpion Ltd

DOI 10.1070/RC2013v082n03ABEH004278

NMR methods for studying ion and molecular transport in polymer electrolytes

V I Volkov, A A Marinin

Contents

I.	Introduction	248
II.	Ion-exchange membranes and polymer electrolytes for lithium cells: main types, composition, structure and physicochemical properties	250
III.	Specific features of cation hydration. Mechanism of cation – functional group interaction	252
IV.	NMR Spectroscopy of polymer electrolytes for lithium cells. Specific features of lithium cation solvation	255
V.	NMR relaxation. Local mobility of molecules and ions	257
VI.	Pulsed field gradient NMR. Diffusion and ionic conductivity	260
VII.	Conclusion	268

Abstract. Data demonstrating the potential of NMR methods in studying the formation of transport channels, the mechanisms of ion – polymer matrix interaction, the mobility and diffusion of ions and molecules in polymer electrolytes are analyzed and generalized. Ion-exchange membranes with polymer matrices of various chemical types are considered. The translational mobilities of ions measured by pulsed field gradient NMR are compared with the data on ionic conductivity acquired by impedance spectroscopy methods. Attention is focused on the possibilities of NMR methods in studying the state of ions and molecules in electrolytes and also their diffusional mobility on different spatial scales. Based on the NMR data, the mechanisms of ion transport in ion-exchange perfluorinated membranes are proposed. The bibliography includes 182 references.

I. Introduction

Ion-exchange membranes and polymer electrolytes for lithium cells attract keen attention of scientists in view of the development of modern environmentally clean and energy-efficient technologies.

The conventional technologies are based on the methods of mixture separation that employ ion-exchange membranes (chlorine electrolysis, electrodialysis, extraction of metal ions from solutions, separation of water-organic mixtures, *etc*.). The interest in ion-exchange membranes has increased due to the development of alternative energy sources based on fuel cells (FC).

Lithium cells are used for autonomous power supply in various devices such as laptops, cellular phones, digital video cameras, *etc*. and, lately, in automobile, space, aviation and ship-building industries.

The development of highly efficient materials requires fundamental scientific knowledge of the mechanisms of ion and molecular transport. The studies performed in this field so far mainly concerned the macroscopic processes of electro and mass transfer;[1–7] however, elucidation of the mechanism of selective ion and molecular transport requires investigation of diffusion at the microscopic level.

Of most interest is the relationship between the following fundamentally important characteristics that determine the ion and molecular transport.

1. The nanoscale structure of ion transport channels. The structure and dynamics of polymer matrix at the submicrolevel, *i.e*., from several tenths of nanometre (sizes of solvated ions and molecules) to several nanometres or several tens of nanometres (characteristic lateral dimensions and lengths of ionic channels), determine the selective ion transport because these structural units form transport path for ion transfer by macroscopic distances. Studying the nanostructure opens up the prospects for targeted synthesis of polymer electrolytes, insofar as their preparation is accompanied by the formation of the nanostructure.

2. The type of interaction of mobile ions with functional groups and solvating molecules (water, organic compounds) and the state of solvent molecules in the polymer electrolyte. Data on the structure of ionic complexes and also on the mechanisms of interaction of ions and molecules with the polymer matrix are necessary for understanding the mechanisms of selectivity of ion-exchange membranes and elementary steps of the diffusion transport of ions in polymer electrolytes.

3. The elementary steps of diffusion of ions and molecules, which can be characterized by the lifetime of a species

V I Volkov, A A Marinin Institute of Problems of Chemical Physics, Russian Academy of Sciences, prosp. Acad. Semenova 1, 142432 Chernogolovka, Moscow Region, Russian Federation. Tel. (7-496) 522 80 37, e-mail: vitwolf@mail.ru (V I Volkov), prochiy@mail.ru (A A Marinin)

Received 13 October 2011
Uspekhi Khimii **82** (3) 248 – 272 (2013); translated by T Ya Safonova

in a particular state, the time of translational displacement, the partial diffusion coefficient on various spatial scales (if diffusion occurs in a heterogeneous medium or the diffusant consists of different species).

The problem of elementary diffusion jumps logically follows from the aforesaid. Evidently, the time of elementary jump and the height of the potential barrier overcome by a moving species are largely determined by the geometry of diffusion channels and the structure of solvate ionic complexes. This information is necessary for both the elaboration of adequate transport models and the targeted synthesis of high-performance polymer electrolytes.

Highly attractive methods that allow the mentioned information to be acquired are the magnetic resonance methods, particularly, NMR. The main advantage of these methods is the possibility of studying the structural and dynamic properties over a wide spatial scale and in wide ranges of molecular motion frequencies in systems under real conditions.

Analysis of literature data on the state and mobility of ions and molecules in electrolyte solutions, viscous liquids, biological objects, glasses, zeolites and polymer electrolytes made it possible to single out the following possibilities of the most popular magnetic resonance techniques.

Electron paramagnetic resonance (**EPR**) provides information on the composition and structure of the first coordination sphere of paramagnetic ions, their mobility and local concentrations. Numerous publications are devoted to EPR studies of ion exchangers, which include perfluorinated sufo cation-exchange membranes.[8–13] For studying ion-exchange membranes, of great interest is the possibility of probing the structure of the polymer matrix by means of a paramagnetic probe.

The method of electron-nuclear double resonance (**ENDOR**) makes it possible to selectively study the structure and dynamics of the environment of a paramagnetic centre in the range from 0.3–0.5 to 1.5 nm.[14–17]

The EPR and ENDOR methods substantially supplement the traditional research technique such as small-angle X-ray scattering[5,18–22] the resolving power of which usually does not exceed 2–2.5 nm. Some scientists[15–17] used EPR and ENDOR methods for acquiring information on the submicrostructure of membranes on a level from 0.5 to 2.0 nm.

The main methods used in studying the state and mobility of ions in polymer electrolytes are NMR spectroscopy and pulsed NMR techniques, in particular, the NMR relaxation and pulsed field gradient NMR.

NMR spectroscopy. The most popular method is ^{1}H NMR, which was used to study KU-1 sulfonate cation exchanger and the corresponding membranes[4,23–27] and also perfluorinated cation-exchange membranes.[28–34] To date, techniques have been developed for recording high-resolution NMR spectra and the main factors that determine the chemical shift of water protons in granulated sulfonate cation-exchangers and ion-exchange membranes have been elucidated. The required information can also be obtained from the solid-state high-resolution NMR spectroscopy data.[33,34] Information on hydration of ionic channels in membranes is of fundamental importance for understanding the mechanism of migration of cations and water molecules.

NMR studies of cations in membranes[30,31,35–38] and in gel and solid electrolytes of lithium cells[39–52] were reported. The possibility of recording ^{7}Li, ^{23}Na and ^{133}Cs NMR spectra for these systems has been demonstrated. The analysis of concentration dependences of chemical shifts and the shapes of NMR lines for these nuclei provided information on the mechanisms of interaction of alkali metal ions with ionogenic groups and on the cation mobility.

Pulse NMR methods. The NMR relaxation methods provide unique information on the mobility of ions and molecules. The first studies of water molecule mobility in granulated sulfonate cation exchanger by the NMR relaxation techniques were carried out more than 50 years ago.[23,38] The quantitative treatment of experimental data was difficult due to the wide distribution of the correlation times of the motion of water molecules and the presence of paramagnetic impurities in these systems. The same drawbacks are inherent in the studies carried out on perfluorinated sulfonate cation-exchange membranes Nafion.[53–59]

The study of the metal ion mobility in polymer electrolytes is associated with even more serious complications. The most serious obstacle is the absence of theoretical works to serve as the base for studying the region of diffusion motion with the characteristic correlation times longer than ω^{-1} (where ω is the NMR frequency, usually, $\sim 10^9$ Hz). To date, ^{7}Li and ^{23}Na NMR relaxation works have been performed dealing with the mobilities of lithium and sodium cations in the KU-2 type sulfonate cation exchangers and the corresponding membranes, perfluorinated sulfonate cation-exchange membranes[57–66] and polymer electrolytes for lithium cells.[67–73]

The pulsed field gradient NMR method,[74,75] which makes it possible to directly measure the diffusion coefficients of protons and other ions in heterogeneous media,† is free from these drawbacks. The number of studies of this type substantially increased in the last decades,[5,6,12,29,57–59,76–106] which was associated with the increased interest in the problems of ionic mobility in polyelectrolytes.

To summarize the foregoing, the following points should be stressed. The magnetic resonance techniques and, especially, NMR methods provide the unique possibility of acquiring detailed information on the state of molecules and ions, the local molecular and ionic mobility and the diffusion on the spatial scale from several tenths of nanometre to several millimetres. The advantages of NMR spectroscopy involve also the possibility of studying one and the same sample under conditions resembling the service conditions by several methods simultaneously, which makes it possible to compare the results of different measurements and unambiguously interpret them. For these studies to be performed, the experimental procedures should be worked out and the problems associated with theoretical quantitative description of data should be solved.

The NMR methods are especially attractive for acquiring detailed information on the ion and molecular transport in polymer electrolytes. The modern level of experimental research instruments allows one to study both elementary processes and macroscopic transfer under the service con-

† In this case, by the diffusion of molecules and ions is meant their spatial displacement in a thermodynamically equilibrium material medium due to random motion.

ditions of electrochemical systems. The successful introduction of NMR methods into the research and technological practice is limited by the lack of publications devoted, first of all, to demonstration of the potential of experimental NMR techniques in this research field.

Despite the considerable number of NMR studies of polymer electrolytes, the reviews on this subject are scarce. In the present review, the experimental results obtained by NMR methods on the ion and molecular transport in polymer electrolytes carried out in Russia and abroad are analyzed and generalized. From our point of view, such an analysis will demonstrate the potential of modern NMR methods and help to reveal some fundamental features of ion and molecular transport in polymer electrolytes at the molecular level.

The main results of NMR studies in ion-exchange membranes and polymer electrolytes for lithium cells are discussed. Attention is focused on the potential of NMR techniques in solving particular problems in relation to the most widely known polymer electrolytes. The most thorough studies were carried out for perfluorinated membranes. Using these membranes as examples, an attempt is made to find the relationship between the polymer matrix structure, the ion solvation details, and the diffusion mobility of ions and molecules on different spatial scales and then to utilize this information for revealing details of the ion transport mechanism in ion-exchange membranes. To our regret, the results obtained by the NMR method in polymer electrolytes of lithium cells are fragmentary due to the wide diversity of materials, their complex structure and the fact that active studies of polymer electrolytes started only ten years ago. In connection with this, the sections devoted to polymer electrolytes are focused on discussing the possibilities of NMR methods in retrieving information on the structure and dynamics of these systems.

II. Ion-exchange membranes and polymer electrolytes for lithium cells: main types, composition, structure and physicochemical properties

1. Ion-exchange membranes

The main studies with the use of NMR methods were carried out on perfluorinated sulfonate cation-exchange membranes Nafion and MF-4SK (Russian analogue of Nafion). At present, the nanostructure of perfluorinated sulfonate cation-exchange membranes has been studied in sufficient detail. Several models were proposed for describing the transport channels[5, 18–22, 107–112] of which the Gierke model[6, 107–109] was used most widely. This model is based on the concept that water molecules and counterions form spherical clusters with walls built of sulfo groups. The clusters are connected by channels. The limiting step of diffusion is ion and molecular transport in the channels. A group of authors[5, 18, 19] proposed the channel model of perfluorinated membranes (Fig. 1).

Based on the data of small-angle X-ray scattering,[18, 19] Mössbauer spectroscopy[111] and standard porosimetry,[112] it was found that associates including sulfo groups, counterions and water molecules are formed in the amorphous part of the membrane. These associates form the ion transport channels with the volume of approximately a fourth of the total membrane volume.[11, 12] The relationship between the polymer matrix structure and the ion and molecular transport will be considered in detail below.

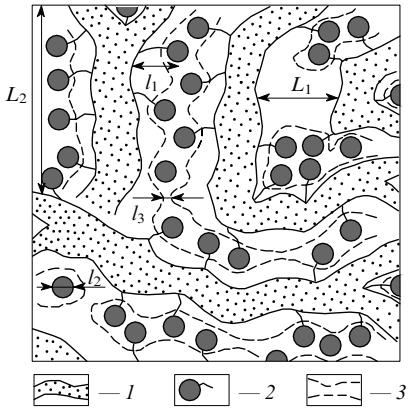


Figure 1. Structure of the amorphous part of a perfluorinated sulfonate cation-exchange membrane.[5]
(*1*) Polymer backbone; (*2*) hydrated counter-ions and functional groups at a low moisture content; (*3*) transport channels for ions and water molecules at a high moisture content; $L_1 = 4$ nm according to low-angle X-ray scattering data; $L_2 = 10$ nm according to Mössbauer spectroscopy; $l_1 = l_2 = 1$ nm according to ENDOR and relaxation NMR data; $l_3 = 1.5$ nm according to standard porosimetry and ENDOR methods.

Another extensive class of membranes are sulfonate cation-exchange membranes based on styrene–divinylbenzene. Both heterogeneous and homogeneous membranes were studied as well as gel and macroporous sulfonate cation exchangers KU-2 and KU-23 and their foreign analogues. The EPR studies of Cu^{2+} cations used as paramagnetic probes revealed two domains containing hydrated copper(II) complexes with different mobility.[8] The dependences of the correlation times and diffusion coefficients of water on the moisture content[76, 77] were consistent with the assumption that the structure of transport channels in such ion exchangers is described by the Gierke model.

Quite promising is a new class of membranes based on aromatic sulfo-containing polyamides.[113, 114] Aromatic polyamides represent rigid-chain polymers with functional groups capable of forming hydrogen bonds both between one another and with sorbed water molecules. Hence, it is important to understand the role of water in the formation of transport channels; according to certain authors (*e.g.*, see Refs 78, 92, 113 and 114), this role is crucial. It was shown that in monosulfo-containing aromatic polyamides, the transport channels are formed by sulfo and amide groups.[78] In bisulfo-containing aromatic polyamides, two types of parallel transport channels are present, those mainly formed by sulfo groups and those mainly formed by amide groups.[92] In view of this fact, it is pertinent to study the diffusional mobility of water and various macromolecules on different spatial scales, first of all, at the molecular level both in aqueous solutions of sulfo-containing aromatic polyamides and in the corresponding polymer films. The results of these studies should be compared with the related data on diffusion transport of metal cations. Sulfonated polynaphthylimides and membranes based on them hold much promise.[115]

Ion-exchange membranes are widely used for separation of water–organic (for the most part, water–alcohol) mix-

tures, particularly, in pervaporation processes. In view of this, in addition to sulfonate cation-exchange membranes, of certain interest are membranes based on polyacrylic acid.[80, 81, 85, 86] Hence, the problem of the mechanism of joint transport of components of water–organic mixtures is challenging, being also associated with development of methanol and ethanol fuel cells.

One of the main requirements imposed on ion-exchange membranes for fuel cells is their high ionic conductivity at a low moisture content. As was shown by studying the electro and mass transfer in membranes of various types, the high mobility of ions and water molecules under these conditions can be reached if polar groups capable of forming the network of additional hydrogen bonds are introduced into channels. One of the methods used for improving the transport characteristics of membranes at a low relative humidity consists in introducing inorganic additives, as was demonstrated for perfluorinated sulfonate cation-exchange membranes Nafion and MF-4SK which are modified with silicon and zirconium oxides and tungsten-containing heteropolyacids.[6, 31, 90, 93, 94] Yet another method is the formation of composite membranes based on, *e.g.*, polyvinyl alcohol and phenolsulfonic acid cross-linked with glutaraldehyde (GA).[88, 116, 117]

The ion transport is related in many respects to the mobility of water molecules and is determined by the character of membrane hydration. To reveal the mechanisms of ionic conduction, it is important to correlate the character of hydration of ionogenic groups with the translational mobility of water molecules and ions and also the electrical conductivity of membranes. Such studies should be carried out for membranes with a well known structure of transport channels.

2. Polymer electrolytes

The leaders in the research and manufacture of lithium cells are Japan, the USA, Korea, France, Germany, Canada and China.[118–120]

The interest in the development of power sources with lithium metal was initiated in the 1960s and the appearance of lithium galvanic cells with aprotic non-aqueous electrolyte solutions dates back to the early 1970s.[121] Besides being compatible with lithium and stable both chemically and electrochemically, a perfect solvent for lithium cells should have high dielectric permittivity and low viscosity, so that the dissolved salt be capable of dissociating into ions and the resulting solution be sufficiently conducting. The most widely used solvents are propylene carbonate, γ-butyrolactone, tetrahydrofuran, dimethyl sulfoxide and thionyl chloride. It is difficult to select a perfect solvent; most frequently, mixed non-aqueous solvents with minimized opposite effects of viscosity and dielectric permittivity on the specific conductivity are used. Many lithium salts, *e.g.*, halides, are usually insoluble in non-aqueous solutions; this is why various intricate lithium complexes with high solubility are used, *e.g.*, $LiClO_4$, $LiAlCl_4$, $LiBF_4$, $LiPF_6$, $LiAsF_6$, *etc.* Requirements to the solvent purity are very severe.

Lithium rechargeable batteries with liquid non-aqueous electrolyte solutions exhibit high power density but very short lifetimes ($\sim$100 cycles) due to passivation of lithium and formation of dendrites.[122] Compact and easily assembled batteries with polymer electrolytes that are free from the mentioned drawbacks are more promising. The state of the art in the field of synthesis of polymer electrolytes and development of high-performance lithium cells is described in numerous reviews (for example, see Refs 123–126).

Polymer electrolytes are subdivided into three main classes.

1. Solid polymer electrolytes (SPE) polymer–salt. The following sufficiently stringent requirements are placed upon polymers involved in the SPE composition:[127]

— the polymers should contain heteroatoms capable of forming stable complexes with the salt cation thus providing the salt dissociation;

— to provide high mobility of ions at room temperature, the polymer should be amorphous or have possibly low glass transition temperature;

— the polymer should be chemically and electrochemically stable and also able to form strong films.

At present, many well-known aliphatic polymers were considered as the candidates for SPE components but the majority of publications are devoted to polyethylene oxide (PEO). However, this flexible-chain polymer has serious drawbacks that prevent its practical use. One of its drawbacks is the tendency to crystallization. This is the reason for low conductivity of PEO-based systems at room temperature (10^{-6}–10^{-8} Ω^{-1} cm^{-1}).[127] Its conductivity increases to 10^{-4} Ω^{-1} cm^{-1} at 80–100 °C; however, at this temperature the current sources can be used very rarely. In addition to PEO, the following polymers were studied as the potential SPE components: poly(propylene oxide), poly(β-propiolactone), poly(ethylene adipate), poly(alkylene sulfide) and polyphosphazenes. Unfortunately, electrolytes based on these polymers exhibit very low conductivity not exceeding 10^{-6} Ω^{-1} cm^{-1} at 35–90 °C.

2. Polymer gel-electrolytes (PGE). To enhance the electrolyte conductivity, a plasticizing organic solvent with a high melting point and a high dielectric permittivity is added to the polymer–salt system. Such electrolytes are called gel-electrolytes. Typical solvents used in liquid organic electrolytes as the plasticizers are listed above.

Polymer gel-electrolytes are subdivided into two classes, namely, homogeneous and heterogeneous. The former are prepared by chemical cross-linking of the polymer matrix in a liquid organic electrolyte medium; the latter are synthesized by preliminary formation of the polymer matrix followed by its impregnation with a liquid electrolyte.

The poly(vinylidene difluoride)–hexafluoropropylene (PVDF–HFP) copolymer is used most widely as the matrix in heterogeneous PGE. Unfortunately, in addition to their high conductivity, gel-electrolytes have a serious drawback, the high volatility of organic solvent present in the composition. At present, studies are being carried out on the preparation of PGE resistant to high temperatures (100 °C) and, in parallel, composite polymer electrolytes are being synthesized.

3. Composite polymer electrolytes (CPE). To enhance the conductivity, ceramic fillers are added to the SPE composition. Such systems have substantial advantages over their gel analogues due to the enhanced mechanical properties and higher stability of the electrolyte/electrode interface. It was proposed to introduce inorganic fillers into the PEO-based SPE. During electrolyte synthesis by the rinsing and drying technique, such systems are crystallized; moreover, the introduction of fine powders increases the 'amorphism' of SPE, which is extremely important because the Li^+ ions are transported only in the amorphous phase. The use of oxides makes it possible to introduce additional oxygen ions capable of coordinating Li^+ ions thus creating

routes for lithium transport. In the early studies,[128,129] relatively large (of the order of several micrometres) filler particles (γ-$LiAlO_2$, Al_2O_3, β-alumina and also $Li_2O-B_2O_3-SiO_2$ ionic glass) were used. Due to the small surface-to-volume ratio of such filler particles, only a small increase in electrolyte conductivity was observed. With the development of nanotechnologies, scientists started to prepare nanosized inorganic fillers for SPE. Thus, promising results were obtained with nanosized particles of Al_2O_3, TiO_2, SiO_2.[130,131] Such SPE are called nanocomposite polymer electrolytes (nano-CPE). Despite the progress in the field of their synthesis, the mechanism of the effect of nanoparticles on the ionic conductivity of polymer electrolyte is still not enirely clear.

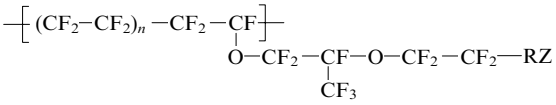
The synthesis of new SPE with desired properties and their efficient use require that the relationship be found between the polymer matrix structure, the specific features of ion solvation, the structure of transport channels and the parameters of electro and mass transfer, in particular, between the ionic conductivity and the translational mobility of ions and molecules. The method of impedance spectroscopy[132,133] makes it possible to measure the integral ionic conductivity but fails to provide information on charge carriers. An important advantage of NMR methods, especially, pulsed field gradient NMR, is the possibility to selectively measure the diffusion coefficients of all ions and molecules involved in charge transfer, for example, of solvents (^{1}H and ^{13}C NMR), lithium cations (^{7}Li NMR) and anions (^{11}B and ^{19}F NMR).

III. Specific features of cation hydration. Mechanism of cation–functional group interaction

The majority of studies of cation hydration were performed by high-resolution ^{1}H NMR. The study objects were first of all sulfonate cation-exchange resins and membranes based on the copolymer of styrene and divinylbenzene and also perfluorinated ion-exchange membranes. Ion exchangers turned out to be so interesting objects that the studies of the state and mobility of water molecules and ions in these systems were started almost immediately after the synthesis of the first ion-exchange resins Dowex and their Russian analogues KU-2 and the appearance of the first commercial NMR spectrometers in the early 1960s.‡

1. ^{1}H NMR spectroscopy

The most thoroughly studied membranes are perfluorinated sulfonate cation-exchange membranes MF-4SK,[28–33] MF-4SK membranes modified with inorganic dopants[31] and perfluorinated carboxylic membranes F-4KF in various ionic forms.[30,31]



R = SO_3 for MF-4SK and Nafion 117; R = CO_2 for F-4KF;
Z = H, Li, Na, Cs

‡ In the USSR, these studies were initiated by N I Nikolaev (L Ya Karpov Physicochemical Institute, Moscow) and V V Mank (Institute of Colloid Chemistry and Chemistry of Water, Academy of Sciences of the Ukrainian SSR, Kiev).

The typical NMR spectra of protons in a perfluorinated sulfonate cation exchange membrane in its Li^+ form and also of hydrated H^+ cations measured at various relative humidity of the environment are rather narrow singlet lines, indicating high mobility of water molecules and H^+ counter-ions in membranes.

As the moisture content decreases, the NMR spectral lines shift downfield for membranes in the acidic form and upfield for membranes in the salt form relative to those of free water. Such changes in the chemical shifts of water protons are associated with the destruction of the hydrogen-bond network in the salt-form membranes and strengthening of hydrogen bonds as a result of hydration of H^+ counter-ions. Figures 2 and 3 show the dependences of the chemical shift on the moisture content of the membranes.

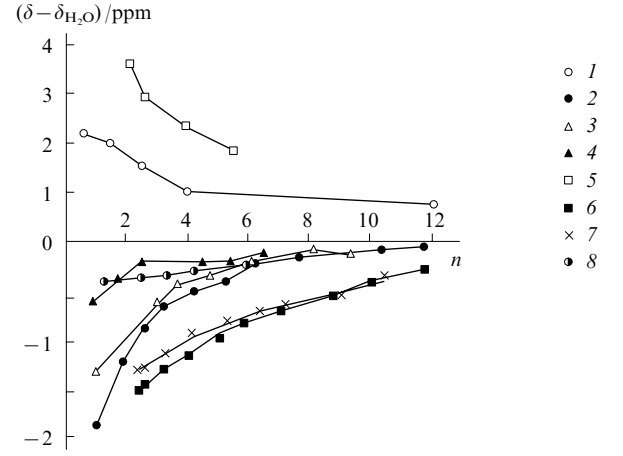


Figure 2. Chemical shift (δ) difference between water protons in the membrane and in liquid water as a function of the moisture content of MF-4SK (*1–4*) and F-4KF (*5–8*) membranes in various ionic forms.[30]
Membrane ionic form: (*1*, *5*) H^+, (*2*, *6*) Li^+, (*3*, *7*) Na^+, (*4*, *8*) Cs^+.

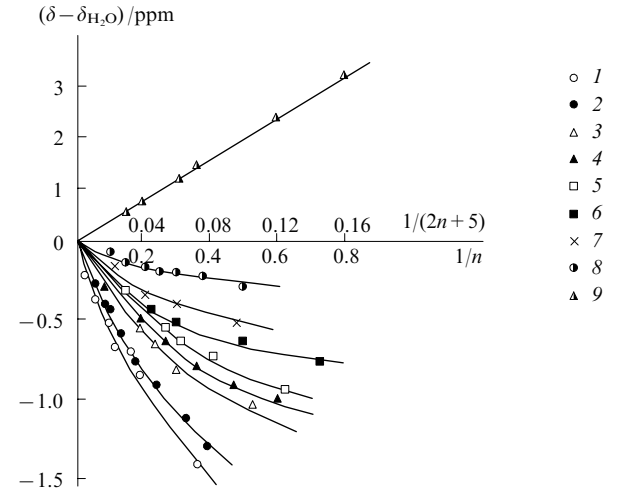


Figure 3. Dependences of chemical shifts of water on the moisture content of MF-4SK membrane.[29]
Membrane ionic form: (*1*) Li^+, (*2*) Na^+, (*3*) K^+, (*4*) Rb^+, (*5*) Cs^+, (*6*) Ba^{2+}, (*7*) Ca^{2+}, (*8*) Mg^{2+}, (*9*) H^+.

The moisture content measured by gravimetry is expressed as the number of water molecules (n) per ionogenic group.

The ^{1}H chemical shifts sharply change starting from a certain critical value n because at a low water content, all water molecules occupy the first hydration shell of the cation and are strongly affected by the cation. The hydration energy of H^+, Li^+ and Na^+ cations is higher and the hydration energy of Cs^+ is lower than the hydrogen bond energy; hence, the changes in the chemical shifts of water protons are not so pronounced in Cs films.

The calculated hydration numbers [the average number of water molecules in the hydration shell of an ion (h_0)] are as follows:

for perfluorinated membranes (±0.5)

H^+	Li^+	Na^+	Cs^+
2.3	3.8	3.5	1.7

for carboxylic membranes (±0.5)

H^+	Li^+	Na^+	Cs^+
1.3	2.8	2	1

The hydration numbers for Li^+, Na^+ and Cs^+ were also assessed from the dependences of ^{7}Li, ^{23}Na and ^{133}Cs chemical shifts on the moisture content. These values well agree with the data of proton magnetic resonance.

In the air-dry acidic form of sulfonate cation exchange membranes, each of the two remaining water molecules forms the stable cation $H_5O_2^+$ with the counter-ion H^+. The observed dependence of the chemical shift on the real fraction of water protons in the membrane $1/(2n+5)$ is a straight line (line *9* in Fig. 3).[29]

The hydration numbers of cations in carboxylic membranes are smaller than in sulfonate cation exchange membranes. This is probably associated with the fact that in F-4SK membranes, the hydration shell of cations includes, first of all, carboxyl groups, whereas in MF-4SK membranes even at $n \approx h_0$ the local environment of a cation contains only water molecules.

It should be noted that the hydration numbers of doubly charged ions substantially exceed those of singly charged ions. In the membranes with a different polymer matrix and, correspondingly, a different structure of transport channels, for instance, styrene–divinylbenzene systems, the hydration is of the same nature. Particularly, the hydration numbers of cations in the Dowex sulfonate cation exchanger found from the temperature dependence of proton chemical shifts are as follows:[134–136]

H^+	Na^+	K^+	Rb^+	Cs^+	Mg^{2+}
2.9	2.9	2.7	2.6	3.2	6.7

It can be seen that the hydration numbers for the same cations in membranes based on polymer matrices of different chemical nature found by different methods are close to one another. This fact and also the weak dependence of the chemical shift in electrolyte solutions on the type of anion suggest that in cation-exchange membranes, water molecules interact mainly with cations. The fraction of cleaved hydrogen bonds (compared with free water) increases with increase in the hydration energy of cations.[29]

For $n > h_0$, the cation and the functional group form a solvent-separated ion pair and the hydration shells of ionogenic groups overlap (Fig. 4*a*). For a low moisture content $n < h_0$, the network of hydrogen bonds between water molecules is broken thus hampering the ion hopping between the neighbouring ionogenic groups (Fig. 4*b*).

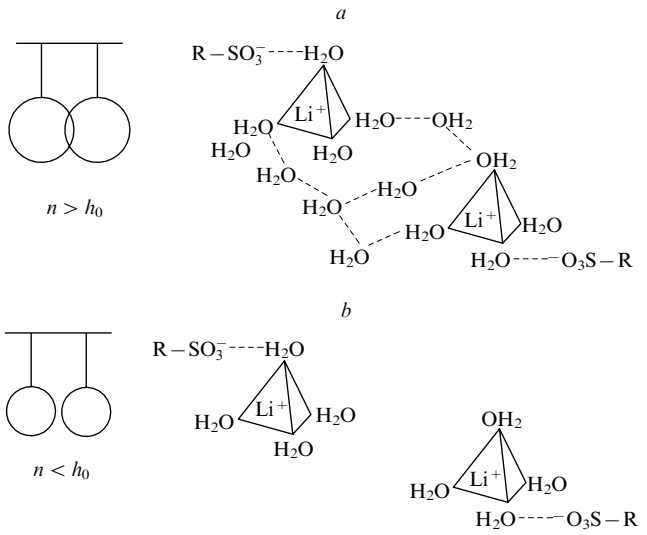


Figure 4. Illustration of hydration of functional groups in the salt forms of MF-4SK membranes by the example of its Li^+-form.[58]

As was mentioned above, one of requirements imposed on membranes for fuel cells is the high ionic conductivity for the low moisture content. To make this true, it is necessary to form a continuous network of hydrogen bonds at a low number n. Several ways have been proposed for solving this problem:

— modification of perfluorinated cation-exchange membranes by introducing dopants that serve as additional sites for sorption of water molecules;

— development of composite membranes based on proton-generating components and polymers with polar hydrophilic groups.

The first way was considered in detail.[6, 31, 90, 93, 94] The introduction of silicon dioxide and heteropoly compounds into MF-4SK membranes led to the displacement of chemical shifts to the region of high moisture contents for one and the same relative humidity (RH) (Table 1). This indicated that inorganic dopants can serve as additional sites for water sorption, which results in formation of a network of hydrogen bonds at a low moisture content. As a result of this modification, the conductivity of membranes increased. A similar effect was observed for Nafion membranes.[33]

In contrast to perfluorinated sulfonate cation exchange membranes, in polyamide systems the chemical shift of water was found to be virtually independent of the moisture content and displaced downfield.

For aromatic polyamides, the downfield shift of the proton signals occurs due to additional binding of water molecules to the polar carbonyl and amide groups of the polymer matrix to form extra hydrogen bonds. The number of water molecules bound to a cation is much smaller as compared with perfluorinated sulfonate cation exchange membranes, which manifests itself as the weak dependence of the chemical shift on the moisture content.[30]

Table 1. ^{1}H chemical shifts in original and modified MF-4SK membranes in various ionic forms.[31]

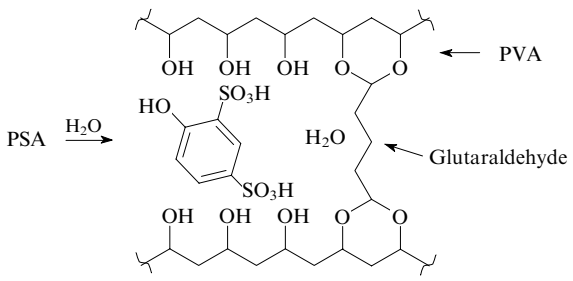
Ionic form	RH (%)	δ ^{1}(H)/ppm			
		I	II	III	IV
H^+	95	5.38	5.29	5.62	5.21
	75	5.86	6.02	6.04	5.31
	58	6.10	6.27	6.35	5.50
	32	6.55	6.39	6.53	5.61
	10	6.78	6.50	6.69	5.74
Li^+	95	4.14	4.18	3.85	4.19
	75	3.90	3.87	3.83	3.88
	58	3.81	3.82	3.82	3.78
	32	3.69	3.75	3.78	3.62
	10	3.45	3.63	3.63	3.52
Na^+	95	3.96	3.74	3.74	3.92
	75	3.77	3.61	3.61	3.52
	58	3.44	3.28	3.42	3.27
	32	3.21	3.14	3.33	3.12
	10	3.12	3.01	3.21	2.96
Cs^+	95	3.78	4.04	3.62	3.51
	75	3.42	3.27	3.31	3.30
	58	3.18	3.15	3.19	3.51
	32	3.09	2.94	3.04	3.42
	10	3.00	2.80	2.90	3.30

Note. The following designations are used for membranes: I is MF-4SK; II is MF-4SK + SiO_2; III is MF-4SK + SiO_2 + $H_3PW_{12}O_{40}$; IV is MF-4SK + SiO_2 + $Cs_xH_{3-x}PW_{12}O_{40}$.

2. Potential of the solid state NMR method in studying ion-exchange membranes of complex composition

An attempt was undertaken[112] to study the structure and the hydration processes in composite membranes based on polyvinyl alcohol (PVA) and phenol-2,4-disulfonic acid (PSA) as a function of their composition, degree of cross-linking and moisture content. ^{1}H NMR and ^{13}C NMR techniques with magic angle spinning of the sample allowed high-resolution spectra to be recorded for both the polymer matrix and the immobile proton-generating additive.

The ^{1}H NMR spectra contain signals of protons of PSA aromatic rings, hydrated H^+ counter-ions and protons of OH groups in PVA, which produced an intense peak at 6.7 ppm due to the fast molecular exchange, and also of CH and CH_2 groups of the alcohol. The procedure of magic angle spinning of the sample favoured the good resolution on ^{13}C nuclei, which made it possible to study the structure and dynamics of the polymer matrix.[117]



Based on the data of analysis of the proton spectra of PVA/PSA membranes, it is possible to calculate the solvate complex parameters. Fast exchange apparently occurs between the H^+ counter-ions, protons of water molecules and, in our case, probably, OH protons of PVA and PSA. The exchange frequency exceeds the difference between resonance frequencies of individual components; hence, the signal in the spectrum of hydrated (solvated) H^+ counter-ions represents a singlet line. The observed chemical shift is equal to the weighted average sum of chemical shifts of protons present in the molecular structures $H^+[(H_2O)_n](H_2O)_n(OH)_m$.

For low moisture content and as the PVA fraction increases, the PSA hydroxyl groups take part in the formation of an additional network of hydrogen bonds. This very fact explains the high proton conductivity in these membranes under mentioned conditions.

3. ^{7}Li, ^{23}Na and ^{133}Cs NMR spectroscopy. Mechanisms of cation–ionogenic group interaction

Figure 5 shows the dependences of chemical shifts in ^{7}Li NMR spectra on the moisture content in the Li^+ form of MF-4SK, Nafion 117, and carboxylic F-4KF membranes.

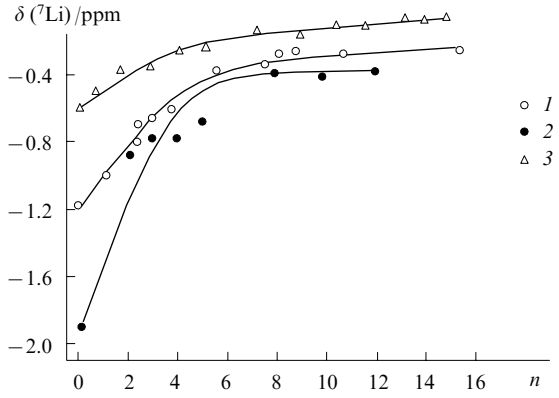


Figure 5. Dependences of chemical shifts in ^{7}Li NMR spectra on the moisture content of the Li^+ forms of perfluorinated sulfonate cation-exchange membranes MF-4SK (*1*), Nafion 117 (*2*) and carboxylic membranes F-4KF (*3*).[30, 31]

For $n > 4$, the chemical shifts depend slightly on the membrane type and the moisture content; for $n < 4$, the ^{7}Li chemical shift for sulfonate cation exchange membranes begins to decrease. The half-widths of ^{7}Li NMR lines at $n > 3-4$ are almost the same for all membranes, while their sharp increase is observed at $n < 2-3$ which is associated with the longer lifetimes of Li^+ ions located on ionogenic groups.

The dependences of chemical shifts on the moisture content in the Na^+ form of MF-4SK and F-4KF membranes (Fig. 6 *a*) are similar to the corresponding dependences for their Li^+ form. For $n > 4-5$, the ^{23}Na chemical shifts are close for sulfonate cation-exchange and carboxylic membranes and start to dramatically decrease at $n < 4-5$. As in the case of Li^+ ions, this can be attributed to the formation of ionogenic group–cation contact pairs, which sharply reduces the sodium ion mobility.

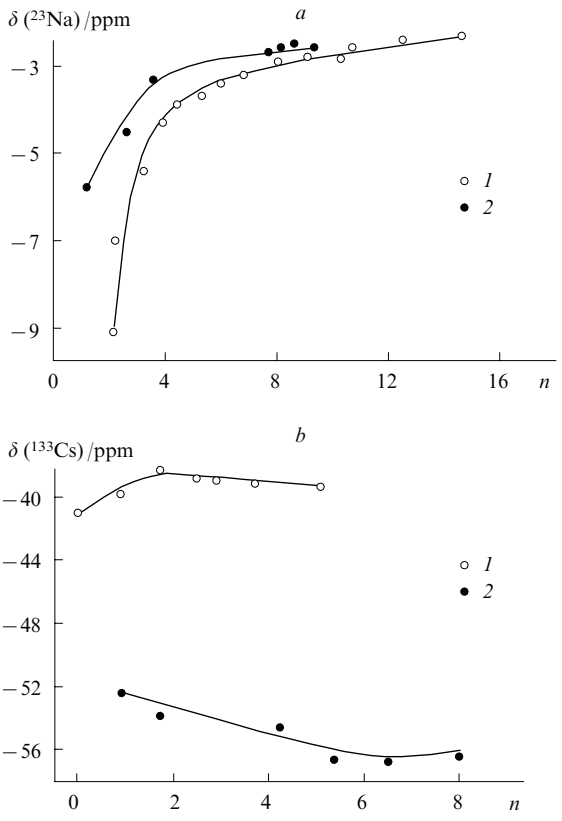


Figure 6. Chemical shifts in ^{23}Na NMR (*a*) and ^{133}Cs NMR (*b*) spectra *vs*. the moisture content of perfluorinated sulfonate cation-exchange membranes MF-4SK (*1*) and carboxylic membranes F-4KF (*2*).[30, 31]

For Cs^+ ion, in contrast to Li^+ and Na^+, the dependences of chemical shifts of NMR lines on the moisture content are far less pronounced (Fig. 6*b*).

Note that for carboxylic membranes, the signals are shifted more upfield than those of sulfonate cation-exchange membranes (see Fig. 6). The slight effect of the moisture content on the chemical shift and the half-width of ^{133}Cs NMR lines can be explained by the above-mentioned peculiarity of hydration of caesium ions, namely, in contrast to Li^+ and Na^+, in the case of Cs^+, the energy of cation–water interaction is lower than the energy of a hydrogen bond between water molecules (negative hydration). This circumstance and also the large crystallographic radius of Cs^+ explain the fact that even at the high moisture contents, water molecules form their own network of hydrogen bonds thus driving out the cations to the periphery. Then, Cs^+ ions and ionogenic groups can directly interact with one another at any degree of hydration. From our point of view, this explains why the local environment of Cs^+ changes only insignificantly upon variation of the moisture content, which is manifested by the weak dependences of the chemical shift and the NMR line half-width on the number of water molecules per ionogenic group.

The observed dependences of chemical shifts and NMR line half-widths on the moisture content can be interpreted as follows. For $n \gg h_0$, the hydrate environment of cations is similar to that observed in aqueous solutions of their salts and the chemical shifts approach those obtained from the $\delta(n)$ dependences at $n \to \infty$. Under these conditions, the counter-ion and the ionogenic group form a solvent-separated ion pair. If water molecules are too few to fill the coordination sphere of an ion ($n < h_0$), then SO_3^- or CO_2^- groups are likely to enter its environment. The formation of such contact ion pairs distorts the symmetry of the hydration shell so that the frequencies of translational motion of ions decrease. Both these factors increase the chemical shifts and the widths of NMR lines for alkali metal ions.[30, 31]

The chemical shift of alkali metal nuclei can be calculated by the formula

$$\delta_i = p_c\delta_{ic} + p_b\delta_{ib}$$

where p_c and p_b are the relative fractions of contact and solvent-separated ion pairs, respectively; δ_{ic}, δ_{ib} are the chemical shifts of ions forming either the contact or solvent-separated ion pairs.[31] Using this equation, the dependences of the relative proportion of contact ion pairs on the moisture content were calculated (Fig. 7).

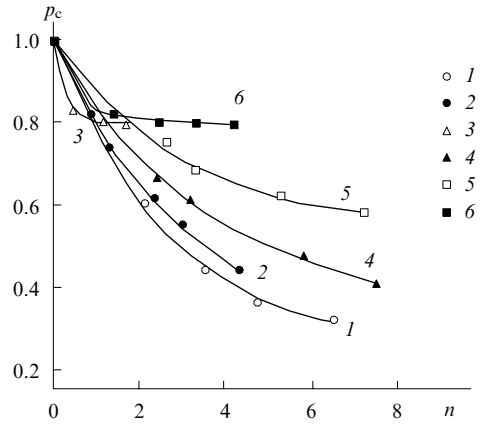


Figure 7. Relative proportion of contact ion pairs *vs*. the moisture content for sulfonate cation-exchange (*1–3*) and carboxylic (*4–6*) membranes in various ionic forms.[30]
Membrane ionic form: (*1*, *4*) Li^+; (*2*, *5*) Na^+; (*3*, *6*) Cs^+.

The fraction of contact ion pairs was found to vary in the following series for both sulfonate cation-exchange and carboxylic membranes:

$$Cs^+ > Na^+ > Li^+.$$

IV. NMR Spectroscopy of polymer electrolytes for lithium cells. Specific features of lithium cation solvation

1. High-resolution NMR spectroscopy

Ethylene carbonate solutions of $LiClO_4$ were studied as polyelectrolyte components by high-resolution ^{1}H, ^{7}Li, ^{13}C, ^{17}O and ^{35}Cl NMR.[39, 40]

In the concentration range from 0.01 to 1 mol litre^{-1}, chemical shifts were observed to be independent of the solution concentration; for concentrations from 2 to 3 mol litre^{-1}, the variations in the chemical shift were apparently due to association of cations and anions. This assumption was confirmed by quantum chemical calculations of solvate

shells of cations and anions, which have demonstrated that the contact ion pairs are formed at solution concentrations of 42 mol litre^{-1}.

For lithium salts dissolved in SPE, the range of ^{7}Li NMR chemical shifts was narrow ($\sim$1 ppm) and comparable with the width of lines for these signals, which complicated the analysis of the Li^+ ion environment.[41] Cations with the larger numbers of outer electrons are more sensitive with respect to such interactions. This was demonstrated, for instance, for hybrid electrolytes based on SiO_2 and propylene oxide with dissolved $NaClO_4$ salt. [42]

2. High-resolution NMR spectroscopy in solids

To exclude the anisotropic part of dipole–dipole interactions and thus reduce the width of spectrum lines, it is the practice to use the magic angle spinning NMR technique;[47] thus, various ion pairs and associates can be detected in polymer electrolytes, which is difficult by other methods.

Hybrid gel electrolytes with addition of tetraethoxysilane were studied.[43] The analysis of magic angle spinning ^{7}Li spectra recorded in the temperature range from -140 to 80 °C has shown that at low temperatures, lithium cations can form complexes with the polymer matrix, whereas at higher temperatures cations are coordinated to solvent molecules.

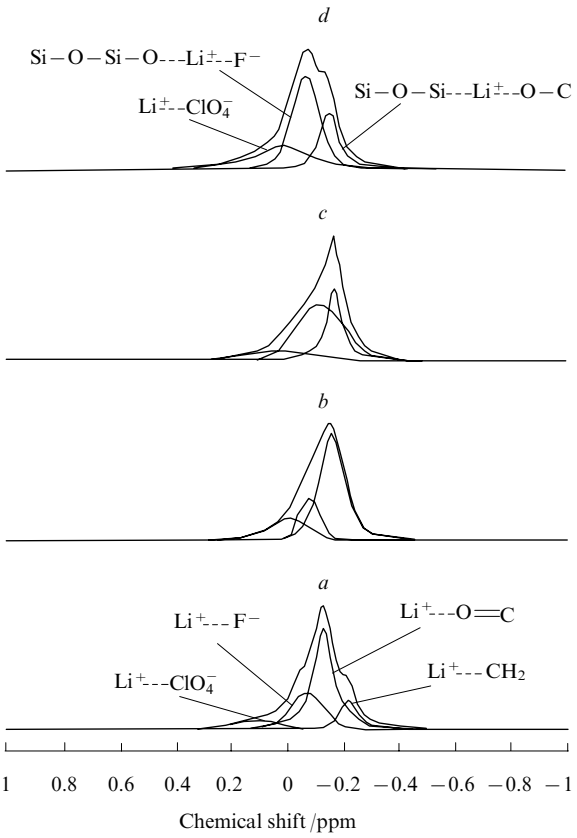


Figure 8. Resolution of the ^{7}Li NMR spectrum for the system (PVDF-HFP)–(PC + EC)–$LiClO_4$–SAG for the following component contents (mass %): 20 : 70 : 10 : 0 (*a*), 20 : 69 : 10 : 1 (*b*), 20 : 66 : 10 : 4 (*c*), 20 : 64 : 10 : 6 (*d*).[44]
The sample spinning frequency is 2 kHz.

The ^{7}Li NMR spectra of composite gel electrolytes based on copolymers of poly(vinylidene difluoride) and hexafluoropropylene with addition of silicate aerogel (SAG) and solvents, namely, ethylene carbonate (EC) and propylene carbonate (PC), can be found in Ref. 44 for different contents of $LiClO_4$ and aerogel (Fig. 8).

As a result of spectrum deconvolution, four components were detected that corresponded to different lithium ion environments in a gel electrolyte containing no SAG. A peak at 0.104 ppm was assigned to ion pairs and aggregates, a peak at 0.07 ppm was attributed to Li^+ cations interacting with fluorine atoms in PVDF–HFP, and peaks at 0.13 and 0.21 ppm corresponded to Li^+ ions coordinated with propylene carbonate and diethyl carbonate, respectively.[45,46] Upon the addition of SAG (12 mass %), the shape and intensity of lines of individual components profoundly changed, which pointed to the interaction between SAG and Li^+ coordinated to solvent molecules and a decrease in the ion pair fraction (this is in agreement with conductivity data).

Analysis of Li^+ NMR spectra has shown that lithium ions interact with SAG, the solvent and PVDF–HPF. These interactions could induce structural changes in polymer chains and favoured the formation of conditions beneficial for the fast motion of Li^+ ions over the surface of SAG particles.

3. Cross-polarization. Crystallinity and amorphism of polymers

The crystalline and amorphous phases of solid polymer electrolytes can be detected by the dependence of cross-polarization ^{13}C NMR spectra on the duration of radio-frequency (RF) pulses. The dependence between the signal intensity and the contact time is determined by the local chemical environment and the dynamic behaviour of systems under study. The cross-polarization ^{13}C NMR technique makes it possible to separate signals of the crystalline and amorphous polymer phases.

Köster and van Wüllen [49] studied solid polymer electrolytes based on $(PEO)_nLiN(CF_3SO_2)_2$ with $3 \leqslant n \leqslant 20$ by using differential scanning calorimetry (DSC) and X-ray diffraction and also by solid-state NMR, which is suitable to distinguish the mobile and immobile cations and anions and provides information on the polymer electrolyte structure.

For $(PEO)_3LiN(CF_3SO_2)_2$ and $(PEO)_6LiN(CF_3SO_2)_2$ polymer electrolytes, the shape of cross-polarization ^{13}C NMR lines was independent of the contact time, which confirmed the crystalline structure of these samples and was consistent with DSC data. The analysis of the shape of ^{7}Li NMR lines demonstrated the presence of an amorphous phase in the $(PEO)_6LiN(CF_3SO_2)_2$ polymer electrolyte, whereas no such phase was detected by cross-polarization ^{13}C NMR studies. These disagreement could be caused by the fact that due to the small amorphous phase fraction ($\sim$16%), its signal was not detected.

The ^{13}C NMR spectra of the $(PEO)_3LiN(CF_3SO_2)_2$ system contained a single line, which suggested that carbon atoms in the polymer electrolyte occupied equivalent crystallographic sites. In contrast, the ^{13}C NMR spectra of the $(PEO)_6LiN(CF_3SO_2)_2$ system contained several unresolved lines. The spectral lines of this sample could correspond to carbon atoms in different crystallographic sites. The spectra of pure poly(ethylene oxide) represent superpositions of a

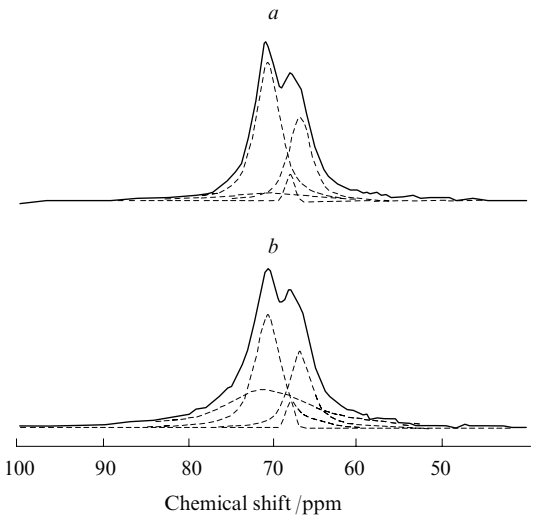


Figure 9. $^{13}C-\{^1H\}$ cross polarization NMR spectra for $(PEO)_{10}LiN(CF_3SO_2)_2$ polymer electrolyte.[49]
Contact time 1 (*a*) and 0.25 ms (*b*).

narrow line of the crystalline phase and a wide line of the amorphous phase.

Of special interest is the $(PEO)_{10}LiN(CF_3SO_2)_2$ polymer electrolyte. Based on DSC data and analysis of temperature dependences of ^7Li and ^{19}F NMR spectra, it was assumed that this electrolyte is totally amorphous and, hence, it should exhibit high ionic conductivity. However, according to Fig. 9, the pattern of the spectrum composed of many lines depends on the contact time. For long-term contacts, the signals with chemical shifts at 66 and 70 ppm are associated with the presence of the $(PEO)_6LiN(CF_3SO_2)_2$ polyelectrolyte, *i.e.*, a crystalline phase, in $(PEO)_{10}LiN.(CF_3SO_2)_2$. For short-term contacts, a wide line was observed, which can be attributed to the amorphous phase.

4. Determination of internuclear distances by the rotational echo double resonance technique

Analysis of the spin echo signal obtained at magic angle spinning under conditions of double resonance [rotational echo double resonance (REDOR) signal] makes it possible to assess the dipole–dipole interaction between nuclei and calculate internuclear distances.[50] For structural studies, it is of interest to consider heteronuclear interactions.[137] Andreev *et al.*[51] determined the magnitude of the dipole–dipole interaction between ^{13}C and ^7Li nuclei in PEO to be 358 Hz, which corresponds to the internuclear distance of 3.15 ± 0.2 Å. This value agree with X-ray diffraction data ($\langle d_{C-Li} \rangle = 3.10$ Å) and with the REDOR–NMR data for $(PEO)_6LiPF_6$ (3.2 Å).[138]

Neutron scattering techniques and REDOR provide similar values of internuclear distances for standard structures (for instance, lithium acetate dihydrate) but there are some discrepancies for crystalline $(PEO)_6LiPF_6$. The Li–C distance determined from the REDOR–NMR spectra is ~3.14 Å, whereas the corresponding value found from a neutron diffraction experiment fits the range from 2.23 to 4.27 Å.[139] These results point to certain specifics and limitations of this method. Even in crystalline SPE, the distribution of internuclear distances is sufficiently wide, so that in amorphous SPE their distribution can be assumed to be even wider. The use of the REDOR–NMR method assumes the presence of a strong dipole–dipole interaction between the examined nuclei and so strong interaction can be observed only in crystalline samples or in samples with a high degree of crystallinity. Probably, the new modified techniques such as REREDOR (Rotor Encoded REDOR) will help to overcome this limitation and to study systems with high mobility and weak dipole–dipole interactions.[52]

V. NMR relaxation. Local mobility of molecules and ions

Despite considerable progress in the research of ion and molecular transport in polymers electrolytes, the microscale transfer mechanisms are still unclear. As was stated above, the NMR methods furnish a lot of information on the local motion of ions, solvent molecules and polymer matrices. The times of spin–lattice (T_1) and spin–spin (T_2) relaxation and also the width of NMR lines depend on the modulation frequencies of local (dipole–dipole and quadrupole) couplings that induce magnetic relaxation. To interpret the measured relaxation times, it is necessary to determine the types of interactions and molecular motions. For nuclei with spin 1/2, the principal relaxation interactions are the magnetic homo- and heteronuclear dipole–dipole couplings. The NMR relaxation for nuclei with spin $> 1/2$, *e.g.* ^7Li, is mainly determined by two mechanisms:

— quadrupole relaxation due to interactions between the quadrupole moment of a nucleus with the fluctuating electric field gradient induced by the charge distribution around this nucleus;

— dipole–dipole relaxation caused by random fluctuations of magnetic moments of nuclei.

The detailed description of mechanisms of magnetic relaxation for ^1H and ^7Li nuclei and details of interpretation of experimental data for perfluorinated ion-exchange membranes can be found in several publications.[56, 57, 59, 65]

1. Mobility of water molecules and ions in ion-exchange systems

The majority of studies on the mobility of water molecules and ions in ion-exchange systems deal with magnetic relaxation of water ^1H nuclei, hydrated H^+ counter-ions and ^7Li, ^{19}F, ^{23}Na ions in Dowex-50 and KU-2 sulfonate cation-exchange and perfluorinated sulfonate cation-exchange membranes.[53–65] Despite the large number of publications in this field, the main conclusions were mostly qualitative. The quantitative assessment of motion parameters (correlation times and activation energies) was complicated due to the presence of paramagnetic impurities capable of modulating the relaxation processes.

The most correct assessment of the mobility of water molecules and the dynamic characteristics of lithium cations was carried out for perfluorinated membranes MF-4SK. The samples were thoroughly cleaned from paramagnetic impurities.[56, 57, 59, 65] It was shown that the magnetic dipole–dipole coupling is the main interaction inducing relaxation of water protons. The magnetic relaxation of ^7Li nuclei is modulated by the $^7Li-^1H$ magnetic dipole–dipole coupling and the quadrupole coupling between lithium nuclei and the electric field gradient. The ^1H relaxation was described in terms of the Bloembergen–Purcell–Pound model, which takes into account the distribution of correlation times in the low-temperature region. The relaxation

was either Gaussian or rectangular (*i.e.*, in a certain interval, the correlation times were virtually constant).[57, 65] The processes of spin–lattice relaxation of ^{7}Li nuclei were determined by rapid librations of water molecules within the cation hydration shell, which allowed their lifetime to be calculated.[65] In contrast to the kinetics of longitudinal magnetization decay, the kinetics of transverse magnetization decay was biexponential.

Detailed analysis of spin–spin relaxation processes was carried out.[65] The spin–spin relaxation was assumed to be modulated by slower motions as compared with librations of water molecules within the hydration shell of a lithium cation. These motions are associated with variations of the electric field gradient on a ^{7}Li nucleus as the latter approaches (or moves away from) a sulfo group. Based on these data, the lifetime of lithium cations on sulfo groups was calculated. The algorithms of calculation of correlation times of water molecules, the lifetimes of lithium hydration shells and lithium cations located on sulfo groups for MF-4SK membranes can be found in several publications.[56, 57, 65] Below, we present the main conclusions made in these publications.

Figure 10 shows temperature dependences of the longitudinal and transverse relaxation rates. The resonance frequencies of ^{1}H and ^{7}Li nuclei and the moisture content of MF-4SK membranes in the Li^+ form can be found in Table 2.

Table 2. Resonance frequencies of ^{1}H and ^{7}Li nuclei and moisture content of tested MF-4SK membranes in their Li^+ and H^+ forms.[57]

Nucleus	Frequency /MHz	n	Curve number in the figure		
			10 *a*	10 *b*	11
^{1}H	9.83	21	*1*, *1′*		*3*
^{1}H	90	21	*2*, *2′*		*2*
^{7}Li	34.97	21	*3*		
^{1}H	9.83	5.4		*1*, *1′*	*4*
^{1}H	34.98	5.4		*2*, *2′*	*5*
^{1}H	300	4.7		*3*	*1*

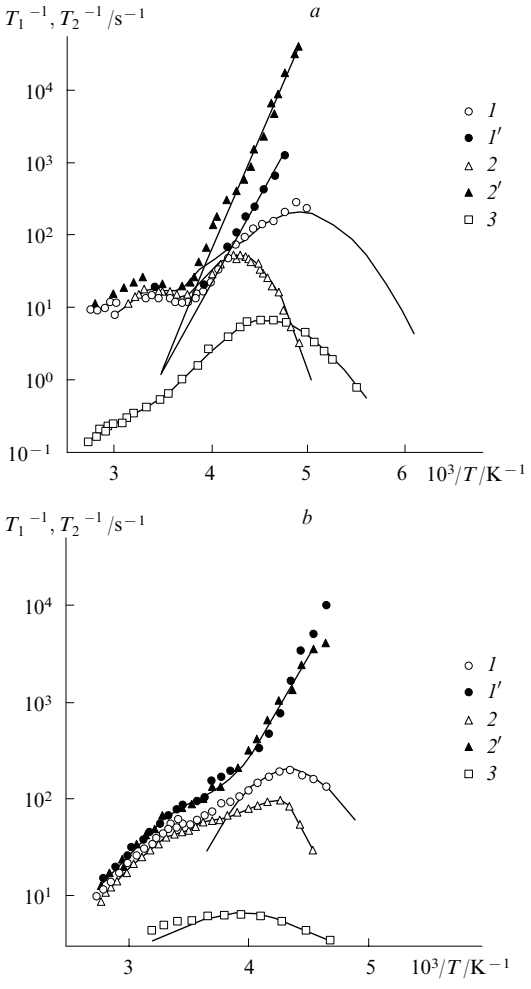


Figure 10. Temperature dependences of the spin–lattice (1–3) and spin–spin relaxation rates (*1′*, *2′*) of the ^{1}H and ^{7}Li nuclei in MF-4SK membranes.[57]
(*1*, *1′*, *2*, *2′*) Li^+ form, (3) H^+ form. NMR frequencies and moisture contents can be found in Table 2.

It was shown that the patterns of motion of water molecules are different in the low- ($T < 280$ K) and high-temperature ($T > 320$ K) ranges. This was associated with the fact that at low temperatures, water molecules form associates that are highly mobile at $T < 0$ °C because in membranes, water molecules interact with charged ionic groups and cannot form the solid phase (ice). In the high-temperature region, water molecules can travel as in electrolyte solutions. In the intermediate temperature range, both phases coexist. Figure 11 shows the temperature dependence of the high-temperature phase population. The transition from one phase to the other is accompanied by energy absorption or evolution due to the formation (rupture) of hydrogen bonds. Note that the observed thermal effect was not associated with freezing (melting) of free water, because according to NMR data, the number of mobile water molecules did not change upon the phase transition.[57]

The calculated (D^{calc}) and experimentally measured (D^{exp}) diffusion coefficients of water and lithium cations

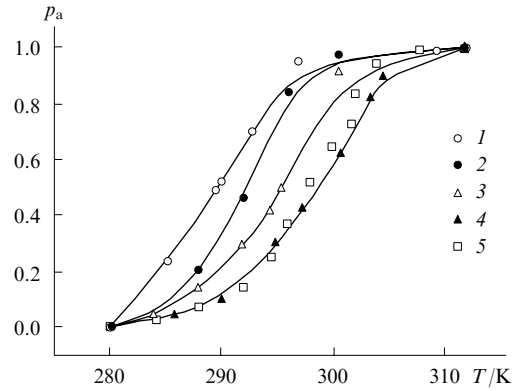


Figure 11. Temperature dependences of population (p_a) of the high-temperature phase for MF-4SK membranes.[57]
For (*1–5*) see Table 2.

($m^2\ s^{-1}$) in MF-4SK membranes with different moisture contents are as follows:

n	$D^{calc}_{H_2O}$	$D^{exp}_{H_2O}$	$D^{calc}_{Li^+}$	$D^{exp}_{Li^+}$
4	5×10^{-12}	4×10^{-12}	2×10^{-12}	10^{-12}
10	3×10^{-10}	2×10^{-10}	4×10^{-11}	3×10^{-11}

There is good agreement between the diffusion coefficients calculated from microscopic mobilities and the macroscopic diffusion coefficients.

Thus, the transfer of ions and molecules by macroscopic distances is controlled by unit jumps of species between neighbouring sulfo groups. This is a fundamental conclusion because, first of all, it confirms the channel model of the MF-4SM membrane structure and, second, it clarifies the interrelation between the peculiarities of membrane hydration and the mass transfer processes.

2. Mobility of ions and molecules in polymer electrolytes for lithium cells

The effect of viscosity on the mobility of ions and molecules in gel-polymer electrolytes based on ethylene glycol, citric acid and lithium perchlorate, which were synthesized by a patented procedure,[140] was studied by NMR, DSC and impedance spectroscopy techniques.[67] The ^{1}H spin–lattice relaxation rate ($1/T_1$) in a gel-polymer electrolyte at temperatures >180 K increased with the increase in temperature and had a maximum (minimum T_1) at 254 K; for sample with the minimum viscosity, $1/T_{1max} \approx 24.5\ s^{-1}$. The presence of the $1/T_1$ maximum unambiguously suggests that in the maximum point

$$\omega\tau_c \approx 1$$

where ω is the NMR frequency, τ_c is the correlation time of relaxation-modulating motions.

Figure 12 shows the temperature dependence of the ^{7}Li spin–lattice relaxation rate. As for protons, the dependence of the longitudinal relaxation rate on the temperature has a maximum; this dependence is symmetrical. As the viscosity increases, the maxima of ^{1}H and ^{7}Li relaxation rates shift to higher temperatures. The correlation times of lithium ion and proton motions were estimated. The temperature dependences of these times followed the Arrhenius plot. A sample of low viscosity was characterized by the lowest correlation times, which indicated that both its segmental and ionic mobilities were fast.

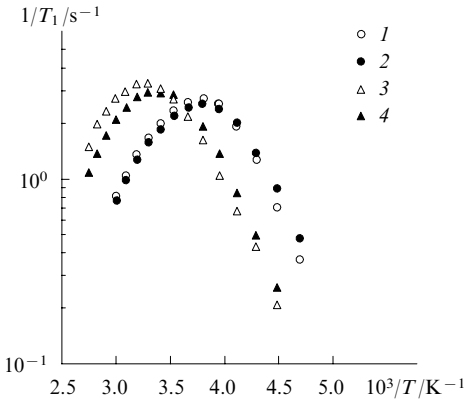


Figure 12. Temperature dependences of spin–lattice relaxation rates for ^{7}Li in the ethylene glycol (EG)–citric acid–lithium perchlorate system measured at the Larmor frequency of 155.4 MHz.[67]
Viscosity/Pa s: (*1*) 197, (*2*) 245, (*3*) 582, (*4*) 868.

The time of spin–spin relaxation for lithium ions reflects the ion mobility ($T_2 \propto \tau_c^{-1}$ in the range $\omega\tau_c \ll 1$); this is why the high T_2 values observed for low-viscosity samples point to the high mobility of lithium cations and, hence, to a high ionic conductivity.

The quantitative description of magnetic relaxation processes in amorphous materials is usually carried out based on the correlation time distribution; hence, the unambiguous determination of mobility parameters is complicated. Under the effect of such distributions, the minimum in the $\omega\tau_c \approx 1$ range broadens and the dependence of time T_1 on the reciprocal temperature has a lower slope than the dependence in the absence of correlation time distribution. Frequently, it is activation energies found based on the NMR relaxation, self-diffusion and conductivity data that are compared; however, it should be borne in mind that conductivity and NMR measurements are performed on different spatial scales, particularly, the NMR relaxation is sensitive to microdynamic motions, while diffusion and conductivity data reflect macroscopic displacements.

The longitudinal ^{1}H, ^{7}Li and ^{19}F NMR relaxation in the electrolyte based on $LiCF_3SO_3$ and poly(ethylene oxide) in the 1 : 4 ratio was studied.[68] In this electrolyte, the minimum T_1 for ^{1}H nuclei was observed in the vicinity of glass transition temperature (T_g) and the minimum spin–lattice relaxation time of ions shifted by 10–15 degrees to lower temperatures. For ^{7}Li and ^{19}F, the T_1 minimum was observed at the same temperature as for pure salt. This can be explained by the fact that the relaxation time of ^{7}Li is determined by the ^{7}Li–^{19}F dipole–dipole coupling, which is modulated by rotations of CF_3 groups. On going from pure salt to its solution in a polymer, the ^{7}Li spin–lattice relaxation time decreases much faster than that for the ^{19}F nuclei.

Based on the data on diffusion and spin–lattice relaxation in a gel-polymer electrolyte formed by a copolymer of poly(ethylene oxide) with poly(propylene oxide), Forsyth *et al.*[69] demonstrated how various solvents affect the ionic conductivity. The minimum time T_1 on ^{7}Li nuclei for a sample containing dimethylformamide (DMF) was much lower as compared with a sample containing propylene carbonate, which can be interpreted as a decrease in the magnetic dipole–dipole coupling induced by the increase in the distance between interacting nuclei (polymer ^{1}H or anion ^{19}F and ^{7}Li). For samples containing PC, the motions were assumed to be more restricted due to the stronger interaction between the cation and the polymer.

The ^{7}Li and ^{19}F spin–spin and spin–lattice relaxation in $LiCF_3SO_3$ dissolved in the amorphous ethylene oxide–propylene oxide co-polymer in the presence of DMF and PC plasticizers were studied.[70] The spin–lattice and spin–spin relaxation times were measured at 13.65 MHz for ^{19}F and 29.6 MHz for ^{7}Li. In the polymer electrolyte containing no solvent, the minimum of the temperature dependence of T_1 (T_1 = 58 ms at 305 K) was observed for ^{7}Li nuclei. Upon the addition of PC, the glass transition temperature

decreased and the relaxation minimum shifted to a low-temperature range.

For non-plasticized polymer electrolytes, the temperature dependence of the longitudinal ^{19}F relaxation time has a clear-cut minimum at 274 K and, probably, a less clear-cut minimum at a lower temperature. For a sample with 20% PC, the second minimum is observed at 156 K.[71] The higher-temperature minimum was attributed to superposition of diffusional and rotational motions of fluorine-containing groups. Data on the conductivity,[141] diffusion [142] and transfer numbers [143] confirmed the assumption that the magnetic relaxation of ^{19}F is due to translational displacements of fluoride anions. The activation energies obtained from temperature dependences of fluorine longitudinal relaxation times are in good agreement with those found from diffusion data.[144]

The ion transport in polymer electrolytes based on $(PEO)_nLiN(CF_3CF_2SO_2)_2$ ($n = 3$, 6, 8, 12 and 20) was studied [72] by impedance spectroscopy and NMR. The shapes of ^1H, ^7Li and ^{19}F NMR and spin–lattice relaxation lines were analyzed in the temperature range from -50 to 100 °C in order to elucidate the polymer electrolyte structure and dynamics. It was shown that with the exclusion of samples with $n = 3$, the width of ^7Li NMR spectrum lines was inversely proportional to the transverse relaxation time and decreased with the increase in temperature. The ^{19}F spectra exhibited two signals for CF_3 and CF_2 groups (Fig. 13), which narrowed down as the concentration of lithium salt decreased. This was associated with weakening of the dipole–dipole coupling because as the salt concentration decreases, the distance between the anions should increase.

Williamson *et al.* [73] studied the ^1H NMR relaxation processes in gel-polymer electrolytes based on poly(vinylidene difluoride) and lithium trifluoromethanesulfonate plasticized with either DMF or tetraethylene glycol dimethyl ether. These data were compared with the results for liquid electrolytes formed by the mentioned solvents. The echo signal decay for liquid electrolytes was well described by single-exponential decay with $T_2 = 348$ ms. For gel-electrolytes, the time dependence of the echo signal had the biexponential form. The slow component for a gel-electrolyte containing DMF was characterized by the time $T_2 = 209$ ms (its weight is 0.64), which pointed to the high mobility of protons in DMF molecules in the liquid phase. The fast component with $T_2 = 48$ ms was associated with less mobile protons in the electrolyte gel phase containing DMF and PVDF molecules. If all protons contributed to the fast component, its weight would be 0.85, which is larger than the experimental value of 0.64. These deviations can be explained by the formation of a solvation shell around the amorphous PVDF regions at the boundary of amorphous and crystalline PVDF phases. A simple model of such partially solvation shell shows that it contains twice more free solvent protons than less mobile protons. These results suggest that gel electrolytes contain a phase similar to the phase of the corresponding liquid electrolytes. This conclusion was confirmed by comparing the diffusion coefficients of the solvent, cations and anions in liquid and gel electrolytes.[145, 146]

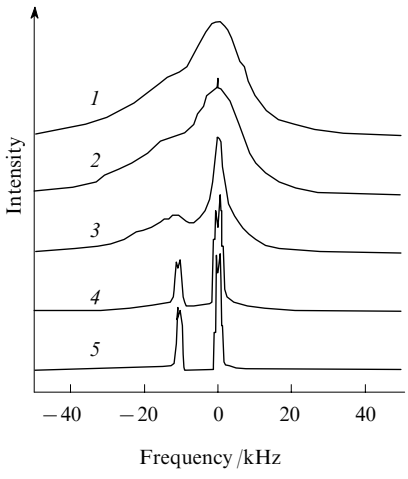


Figure 13. ^{19}F NMR spectra of $(PEO)_3LiN(CF_3CF_2SO_2)_2$ at the following temperatures: -50 (*1*), -20 (*2*), 20 (*3*), 60 (*4*), 90 °C (*5*).[72]

VI. Pulsed field gradient NMR. Diffusion and ionic conductivity

The recent studies of the translational mobility of ions and molecules in ion-exchangers [57–59, 76–106] and polymer electrolytes [47, 147–170] widely employed the pulsed field gradient NMR technique. This method is attractive for studying diffusion because it is suitable for direct measurement of the diffusion coefficients and the relative fractions of the diffusant in different phases of heterogeneous systems. As a rule, the diffusion coefficients are measured by stimulated echo sequences.[74, 75]

The stimulated spin echo signal involves three radio-frequency 90° pulses (Fig. 14). Magnetic field gradients are formed between the first and the second pulses and also after the third RF pulse. Under these conditions, the translational displacement of a species is accompanied by irreversible dephasing of the magnetization vector, which results in a decrease in the spin echo signal amplitude. Conventionally, it is the dependence of the echo signal amplitude (A) on the magnetic field gradient amplitude (g) called the diffusion decay that is analyzed. If for isotropic Brownian diffusion of particles in heterogeneous systems comprising m phases, slow exchange of molecules occurs between the phases, *i.e.*, the diffusion time (t_d) much exceeds the diffusant lifetime in the ith phase

$$t_d = \frac{\Delta - \delta}{3}$$

where Δ is the interval between gradient pulses, δ is the magnetic field gradient pulse duration, then the diffusion decay has the following form:

$$A(g) = A(0)\sum_{i=1}^{m} p_i' \exp(-\gamma^2 g^2 \delta^2 t_d D_i)$$

$$p_i' = p_i \exp\left(\frac{-2t}{T_{2i}} - \frac{t_1}{T_{1i}}\right)\left[\sum_{i=1}^{m} p_i \exp\left(\frac{-2t}{T_{2i}} - \frac{t_1}{T_{1i}}\right)\right]^{-1}$$

$$\sum_{i=1}^{m} p_i = 1, \quad \sum_{i=1}^{m} p_i' = 1$$

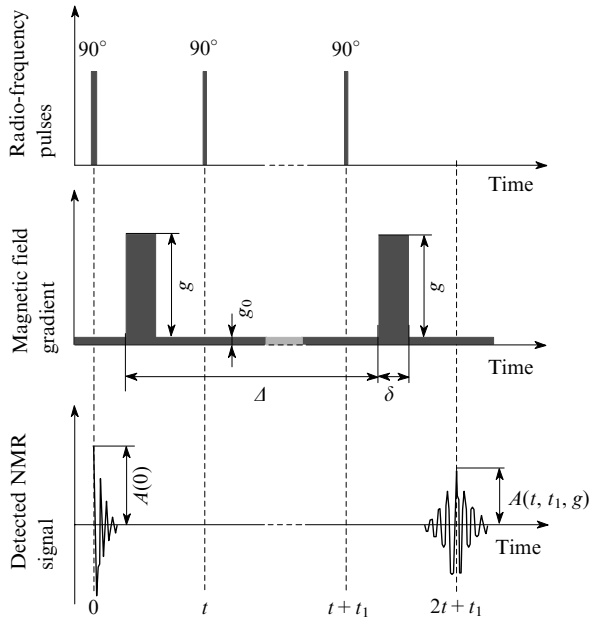


Figure 14. Stimulated spin echo pulse sequence.[75]
t is the interval between the first and the second RF pulses, t_1 is the interval between the second and the third RF pulses, δ is the duration of the magnetic field gradient pulse, Δ is the time interval between the magnetic field gradient pulses, g is the field gradient pulse amplitude.

Here, T_{1i}, T_{2i} are the times of longitudinal and transverse relaxation of water protons in the ith phase, p_i is the relative fraction of molecules in the ith domain (population of the ith phase), γ is the gyromagnetic ratio, D_i is the diffusion coefficient in the ith domain (phase).

By analyzing the $A(g)$ dependence under slow exchange conditions, it is possible to determine the partial diffusion coefficients and the relative proportions of the diffusant molecules in various nano- and microvolumes of membrane systems.

The procedure for calculation of diffusion coefficients in complex polymer electrolytes was described in several publications.[80, 82] The modern NMR spectroscopic instrumentation allows the diffusion coefficient to be measured on various spatial scales starting from several tenths of micrometre; the measurable diffusion coefficients vary from 10^{-14} to 10^{-8} m^2 s^{-1}.

The uniqueness of the pulsed field gradient NMR method lies in the possibility of studying the geometry and permeability of porous media and biological cells. Its idea is based on analysis of how the diffusion decay curve depends on the diffusion time (Fig. 15). For quantitative determination of the limitation size and permeability, the scaling approach was put forward the essence of which is described in several papers.[171, 172]

A substantial drawback restricting the use of pulsed field gradient NMR technique is that it requires sufficiently long (several milliseconds and more) spin – spin relaxation times. This complicates the measurements of diffusion coefficients of ions with quadrulope nuclei (*e.g.*, ^{23}Na, ^{133}Cs). This is why the majority of studies were carried out on the nuclei characterized by sufficiently long transverse relaxation times (^{1}H, ^{7}Li, ^{19}F).

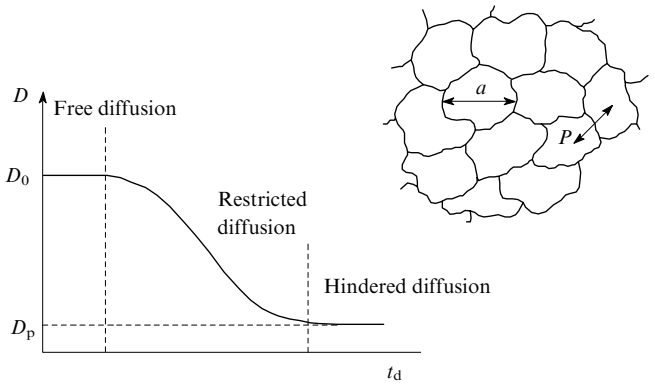


Figure 15. Illustration of the dependence of the apparent diffusion coefficient (D) on time for the case of restricted diffusion.[171]
D_0 is the free diffusion coefficient, D_p is the restricted diffusion coefficient, (a) is the size of restriction regions (pore or cell diameter), $a = (6Dt_d)^{1/2}$; P is the permeability of pore (cell). The shown parameters are interrelated by the following equation:

$$\frac{1}{D_p} = \frac{1}{D_0} + \frac{1}{Pa}.$$

1. Diffusion of ions and molecules in ion-exchange membranes. Relationship between diffusion and conductivity

Now we consider the diffusion of water molecules and alkali metal ions and compare the data on diffusion with conductivity data.[29, 30, 57 – 59, 76 – 106]

Figure 16 *a* shows the dependence of diffusion coefficients of water molecules on the moisture content in perfluorinated membranes of various ionic forms. The diffusion coefficients of water molecules (and hydrated H^+ counter-ions for a membrane in its acidic form) vary in the following sequence of ionic forms for sulfonate cation exchange membranes:

$$H^+ > Cs^+ > Na^+ > Li^+$$

The same series of water diffusion coefficients are typical of carboxylic membranes in the salt form. However, in contrast to MF-4SK membranes, in the acidic form of carboxylic membranes, water and hydrated H^+ cations behave much differently. In carboxylic membranes, the diffusion coefficients are two orders of magnitude smaller than in sulfonate cation-exchange membranes [see curves (*5*) and (*1*) in Fig. 16 *a*]. In carboxylic membranes, restricted diffusion occurs, which is manifested as a decrease in the diffusion coefficients of water and hydrated H^+ cations with increase in the diffusion time (Fig. 16 *b*). The size of restriction regions is ~ 1 μm and decreases with a decrease in the moisture content. Presumably, these restrictions are induced by the formation of internal hydrogen bonds between OH and COO groups of neighbouring macromolecules.

The dependences of ionic conductivity of membranes on the moisture content have a similar form as the analogous dependences for diffusion coefficients.[30] In the region $n < h_0$, the conductivity of samples sharply drops down as the moisture content increases. In sulfonate cation-exchange membranes, the conductivity varies in the following series with the decrease in the ionic radius:

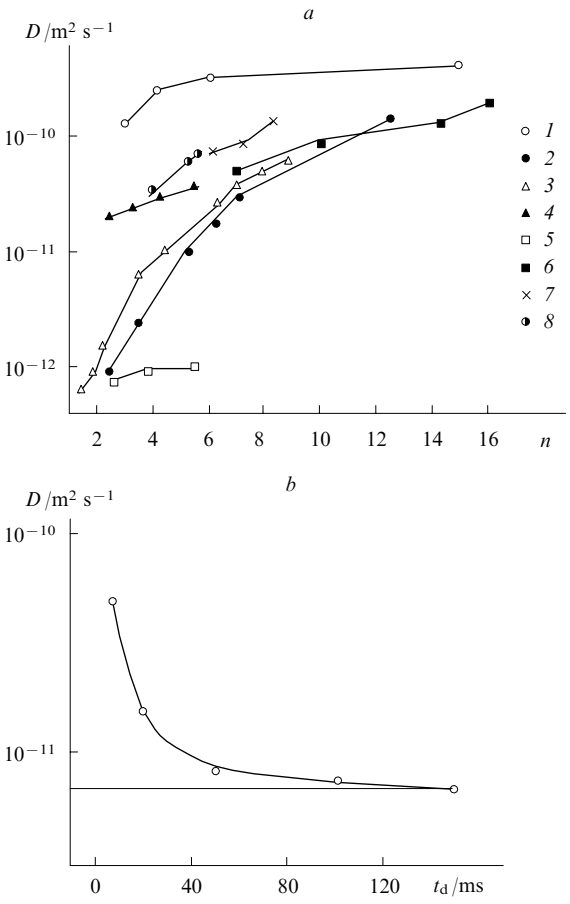


Figure 16. Diffusion coefficients of water molecules *vs.* the moisture content for sulfonate cation-exchange (*1*–*4*) and carboxylic (*5*–*8*) perfluorinated membranes in various ionic forms (*a*) and diffusion coefficients of water molecules and hydrated H^+ counterions in the acidic form of F-4KF membrane *vs.* the diffusion time for the relative humidity of 95% (*b*).[30]
Membrane ionic form: (*1*, *5*) H^+, (*2*, *6*) Li^+, (*3*, *7*) Na^+, (*4*, *8*) Cs^+.

$$Cs^+ > Na^+ > Li^+$$

whereas in carboxylic membranes, the inverse dependence is observed. Sulfonate cation-exchange membranes in their Li^+ and Na^+ forms exhibit higher conductivity as compared with carboxylic membranes. For their Cs^+ form, the inverse dependence was observed. This probably can be explained by the larger radius of caesium ions. The interaction of Cs^+ with the membrane matrix and water molecules is fairly weak even for low degrees of hydration. Moreover, for low degrees of hydration, hopping of caesium cations between the oxygen atoms of ionogenic groups is rather limited by the distance between the oxygen atoms, which is similar for membranes of both types, and not by the negative charge on oxygen ions. For hydroxyl membranes, this distance may be smaller due to a larger negative charge on oxygen atoms.

The conductivity of carboxylic membranes in their acidic form is four orders of magnitude lower than the conductivity of sulfonate membranes in the same form. The data on the conductivity are well correlated with the diffusion data.

Table 3. Ionic conductivities calculated based on diffusion coefficients of water and Li^+ cations and measured for MF-4SK and F-4KF membranes in different ionic forms at the relative humidity of 95%.[30]

Ionic form	$\sigma_{MF\text{-}4SK}$ /S cm^{-1}		$\sigma_{F\text{-}4KF}$ /S cm^{-1}	
	experiment	calculation	experiment	calculation
H^+	2.8×10^{-2}	4.3×10^{-2}	1.5×10^{-7}	1.5×10^{-6}
Li^+	6.2×10^{-3}	1.1×10^{-2} (see [a])	1.0×10^{-3}	4.3×10^{-3}
		6.5×10^{-3} (see [b])		
Na^+	6.1×10^{-3}	1.2×10^{-2}	1.2×10^{-3}	4.6×10^{-3}
Cs^+	3.4×10^{-4}	8.3×10^{-4}	3.7×10^{-4}	7.2×10^{-4}

The calculations were carried out based on diffusion coefficients: [a] water molecules and [b] lithium cations.

The ionic conductivity was calculated based on the Nernst–Einstein equation. The obtained results were compared with the results of direct measurements (Table 3).

For MF-4SK membranes in the Li^+ form, the experimental value of conductivity and the value calculated from diffusion coefficients of lithium cations coincide to within the experimental error (6.2×10^{-3} and 6.5×10^{-3} S cm^{-1}, respectively). The ionic conductivity found from water diffusion coefficients is only several times higher than the conductivity measured experimentally. The similarity of these values suggests that the translational displacements of the cations and water molecules are correlated.

2. Specific features of translational mobility of water molecules and ions at a low moisture content

As mentioned above, the high proton (ionic) conductivity is associated with the presence of a continuous network of hydrogen bonds. The rupture of hydrogen bonds is accompanied by a sharp (threshold) decrease in the mobility of water molecules and cations and in the ionic conductivity.

In accordance with these views on the mechanism of ion transport in ion-exchange systems, the high ion mobility at a low moisture content can be reached by reducing the distance between ionogenic groups. As the concentration of sulfo groups increases, less water molecules are required for hydrogen bonds to be formed. According to Fig. 17, the diffusion coefficients of water at low *n* increase by an order

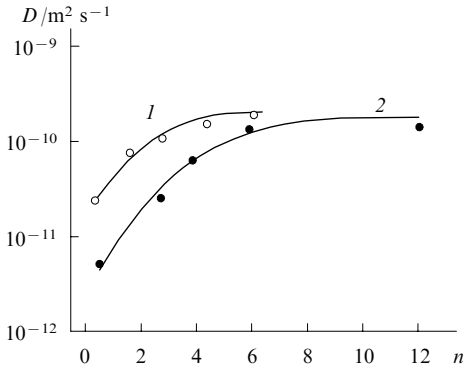


Figure 17. Diffusion coefficients of water on the moisture content in the acidic form of membranes MF-4SK with the exchange capacity of 0.86 (*1*) and 0.34 mg-equiv. g^{-1} (*2*).[58]

of magnitude as the concentration of sulfo groups (exchange capacity) doubles.

Unfortunately, the exchange capacity of membranes cannot be enhanced over a broad range because too high exchange capacities result in sharp deterioration of mechanical properties of the polymer films. In connection with this, as was mentioned above, promising materials are the membranes doped with additional sites for hydrogen sorption or the membranes containing polar hydrophilic groups within their polymer framework.

At low relative humidity, the diffusion coefficients of water and the ionic conductivity for MF-4SK membranes modified with zirconium hydrogen phosphate were shown to be much higher as compared with original unmodified membranes (Fig. 18).[90]

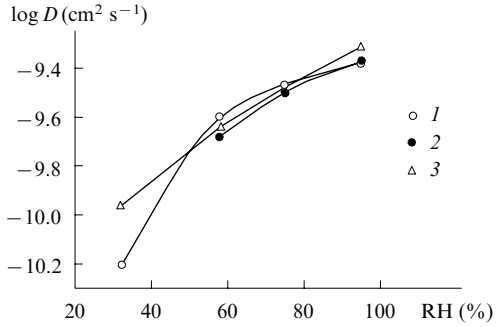


Figure 18. Diffusion coefficients of water *vs*. the relative humidity of MF-4SK membranes: unmodified (*1*), silicon dioxide-modified (*2*) and zirconium hydrogen phosphate-modified (*3*).[90]
The measurements were carried out at 25 °C.

Figure 19 shows the diffusion coefficients of lithium cations in sulfonate membranes with different structures of transport channels and also in isomeric disulfo-containing aromatic polyamides as a function of the moisture content.[30, 58, 95] In systems with amide groups, which serve as bridges reinforcing the network of hydrogen bonds between the sulfo groups, the diffusion coefficients of Li^+ ions are two orders of magnitude higher than in systems containing only sulfo groups (MF-4SK, KU-23). The structure of ionogenic transport channels substantially affects the translational mobility of ions and molecules. Thus, although the exchange capacity of KU-23 is five times higher compared with MF-4SK, the diffusion coefficients of lithium cations in MF-4SK membranes with their uniform distribution of sulfo groups and regular structure of channels were found to be comparable with Li^+ diffusion coefficients in KU-23 in which the transport routes are formed by ionogenic clusters connected by narrow channels (see curves *3*, *4* in Fig. 19). The translational mobility of Li^+ in terephthalic acid having a regular rod-like structure of channels was shown to be higher than in isophthalic acid with a globular packing of polymer chains (see curves *1*, *2* in Fig. 19).

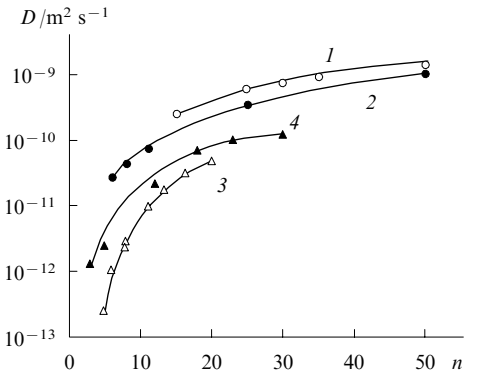


Figure 19. Diffusion coefficients of lithium cations in the system lithium salt–disulfophthalic acid–water [(*1*) is terephthalic, (*2*) is isophthalic] as a function of the moisture content in macroporous sulfonate cation-exchange KU-23 (*4*) and perfluorinated sulfonate cation-exchange membrane MF-4SK (*3*).[92]
Exchange capacity /mg-equiv. g^{-1}: 0.86 for MF-4SK, 5 for macroporous cation exchanger KU-23, 2 for aromatic disulfo-containing polyamides.

Of certain interest is a new class of proton-conducting composite membranes based on polyvinyl alcohol and disulfonic acids. These membranes demonstrated high performance when tested in hydrogen–air fuel cells and hydrogen gas sensors.[116]

As was shown above, at low moisture contents, the alcohol OH groups are incorporated in the solvate complexes formed by H^+ counter-ions, thus creating additional hydrogen bonds which make easier the proton transport.[117] The diffusion of water and H^+ counter-ions in membranes based on PSA and PVA and cross-linked with glutaraldehyde was studied.[88] The comparison of results of NMR experiments with impedance spectroscopy data made it possible to distinguish two types of water molecules with translational mobility differing by an order of magnitude.

As the fraction of PSA was varied, the diffusion coefficient of water molecules with the highest translational mobility decreased by approximately one order of magnitude following the change of the PVA : PSA molar ratio from 4 : 1 to 10 : 1, whereas the diffusion coefficient of less mobile water decreased by almost two orders of magnitude over the same range. The conductivity and mobility variations were similar. The conductivity also decreased with the decrease in the PSA content (Fig. 20).

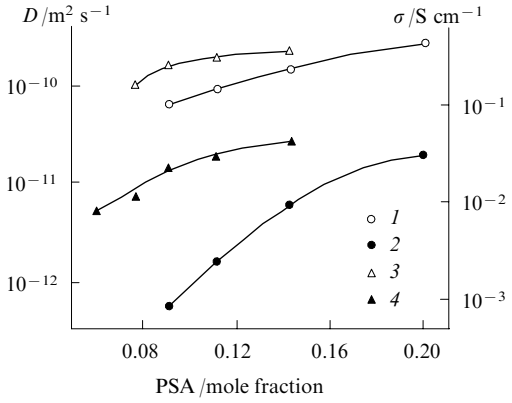


Figure 20. Diffusion coefficients of water (*1*, *2*), diffusion coefficients calculated based on the Nernst–Einstein equation (*3*), and proton conductivity (*4*) in PVA/PSA membranes *vs*. the mole fraction of the acid for 75% relative humidity.[88]

To study the relationship between diffusion and proton conductivity in terms of the Nernst–Einstein equation, the diffusion coefficients were calculated using the impedance spectroscopy results. The fastest water component was shown to be responsible for proton conduction. For high moisture contents, it was assumed that the main contribution to the proton transfer is made by diffusion of hydrated proton complexes.

PVA/PSA films with a 4 : 1 component ratio cross-linked with glutaraldehyde were studied at the relative moisture content of 75%. The amount of cross-linking agent varied from 0.5 mol.% to 4 mol.%. The diffusion coefficients of water and hydrated protons and the proton conductivity were shown to be virtually independent of the amount of glutaraldehyde in the membrane. Figure 21 shows the dependences of diffusion coefficients and proton conductivity on the relative humidity.

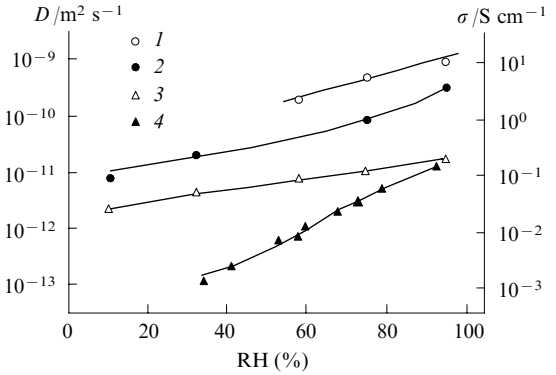


Figure 21. Diffusion coefficients (*1*, *2*) and proton conductivity (*3*, *4*) *vs.* the relative humidity in PVA/PSA (*1–3*) and Nafion (*4*) membranes.[88]
The glutaraldehyde content is 1.5 mol.%.

As can be seen, an increase in relative humidity from 10% to 95% induced the increase in diffusion coefficients by an order of magnitude. Under these conditions, the proton conductivity also increased by an order of magnitude, and at low humidity, it exceeded the conductivity of Nafion membranes by an order of magnitude. This can be explained by interplay of several mechanisms of proton conductivity in the PVA/PSA membrane. For high moisture contents, the main contribution to the proton transfer was assumed to belong to the carrier conduction mechanism. For low moisture contents, the key role is played by the relay-race (Grotthus) mechanism, *i.e.*, hopping along the network of hydrogen bonds involving PSA sulfo groups and PVA hydroxyl groups.

3. Diffusion of saturated monoatomic alcohols and water–alcohol mixtures

The interest in the transfer of organic molecules, especially, alcohols through ion-exchange membranes dates back to the 1980s being associated with the development of the processes of membrane separation of water–organic mixtures. In the past decade, the problem of transport of alcohols became vital for the understanding of processes in methanol and ethanol fuel cells. A lot of publications were devoted to diffusion of saturated monoatomic alcohols and their mixtures in Nafion[97, 100, 101, 105] and MF-4SK membranes,[79, 83, 106] diffusion of water–ethanol solutions through membranes based on mono- and disulfo-containing aromatic polyamides[83] and also through composite polyacrylic acid–polysulfonate membranes.[80]

It was found that unlike water, only a minor portion of alcohol molecules can be located in the hydrophobic regions of perfluorinated MF-4SK membranes, while the major portion remains sorbed in ionogenic channels.

Figure 22 shows the dependences of diffusion coefficients of water, methanol, ethanol and propanol on the number of diffusant molecules per sulfo group in MF-4SK membranes. For the maximum diffusant content, the translational mobility of water molecules is higher as compared with alcohol molecules, whereas in the region of low membrane filling with sorbate molecules, the reverse situation is observed.

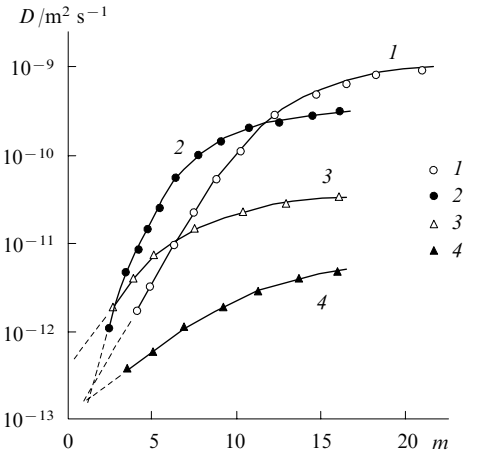


Figure 22. Effect of the diffusant content on the diffusion coefficients of water (*1*), methanol (*2*), ethanol (*3*), propanol (*4*) in the Li^+-form of perfluorinated membrane MF-4SK;[79]
m is the number of diffusant molecules per sulfo group.

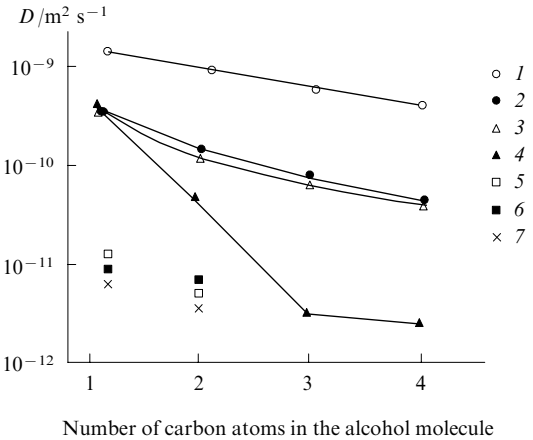


Figure 23. Diffusion coefficients of methanol, ethanol, propanol and butanol in bulk liquids (*1*) and MF-4SK membranes in various ionic forms.[79]
Membrane ionic form: (*2*) Li^+, (*3*) H^+, (*4*) Na^+, (*5*) Cs^+, (*6*) Rb^+, (*7*) K^+.

The diffusion coefficients and diffusion activation energies sharply depend on the ionic form of the membrane and the concentration dependences of diffusion coefficients of alcohols follow a threshold pattern (Figs 22 and 23). Hence, it can be concluded that diffusion of alcohols in MF-4SK membranes is by and large similar to water diffusion.[79]

Translational transfer of alcohols and water molecules in MF-4SK membranes and monosulfo-containing polyamide films proceeds *via* the same ionogenic channels.[83] For this reason, in these systems, the separation factors of water–alcohol mixtures are low.[83] Table 4 shows the partial diffusion coefficients of water and ethanol and the separation factors of their mixture in MF-4SK membranes, films of monosulfo-containing polyamide (PA-1) and disulfo-containing polyamide (PA-2), composite membranes based on polyacrylic acid and polysulfone (PAA–PSF). Apparently, for PA-2 and PAA–PSF, the separation factors are higher by several orders of magnitude as compared with MF-4SK and PA-1. This is associated with the fact that in contrast to MF-4SK and PA-1, the water and ethanol molecules in PA-2 and PAA–PSF are located in different transport channels.[83]

Table 4. Partial diffusion coefficients of water and ethanol and separation factors (α) of their mixture in membranes at 50 °C.[83]

Membrane	$D_{H_2O} \times 10^{10}/m^2\ s^{-1}$	$D_{EtOH} \times 10^{10}/m^2\ s^{-1}$	α
MF-4SK	6	1.5	48
PA-1	0.6	0.15	60
PA-2	40	0.1	10 000
PAA–PSF	1.3	0.026	800

The results concerning the diffusion of water, methanol and ethanol in MF-4SK were supported by later studies devoted to sorption and diffusion of water and methanol in Nafion (Ref. 101) and MF-4SK (Ref. 106) membranes.

4. Diffusion and conductivity in polyelectrolytes for lithium cells

The diffusion of solvent molecules, lithium cations and fluoride anions in liquid electrolytes was studied by pulsed field gradient ^{1}H, ^{7}Li and ^{19}F NMR.[147] The systems under study included a solution of $LiN(CF_3SO_2)_2$ salt in a mixture of propylene carbonate and diethyl carbonate (DEC), another system represented a solution of the same salt in a mixture of PC and 1,2-dimethoxyethane (DME). In the DEC–PC mixture, the diffusion coefficients of both solvents turned out to be virtually the same, whereas in the DME–PC mixture, the translational mobility of DME molecules was higher than that of PC molecules. Usually, solvents diffuse faster in solutions containing no salts due to lower viscosity of such systems. The diffusion coefficients of solvent molecules in salt solutions are higher than diffusion coefficients of cations and anions; also, the translational mobility of fluoride anions is higher than the mobility of lithium cations.

The diffusion coefficients of solvents in systems containing no lithium salts were found to be higher than in the presence of salts, which was attributed to higher viscosity of the systems. The rise of viscosity was observed upon the addition of salt into, *e.g.*, PC and γ-butyrolactone solutions.[151–153]

By comparing the ionic conductivity values calculated based on NMR data with those measured by impedance spectroscopy, the dependences of the degree of dissociation on the concentration were obtained; they were shown to correlate with analogous dependences for salt solutions in polar solvents.[151–153]

Williamson *et al.*[154] used pulsed field gradient ^{1}H, ^{7}Li and ^{19}F NMR to study the dependence of diffusion coefficients of the solvent, Li^+ cations and $CF_3SO_3^-$ anions in solutions of tetraethylene glycol diethyl ether [tetraglyme (TG)] + $LiCF_3SO_3$ and dimethylformamide + $LiCF_3SO_3$ on the temperature and lithium salt concentration. The diffusion coefficients of cations and anions were lower than those of solvent molecules, which was confirmed by more recent data.[149, 151–153] Solvent molecules diffused faster than cations and anions. This was explained by the fact that the experimentally found solvent diffusion coefficients are averaged over two states: the free and the bound ones. The calculated conductivity exceeded the measured value by nearly an order of magnitude. This difference is quantitatively expressed by parameter Δ reflecting the ratio of undissociated ion pairs,

$$\sigma_{exp} = \sigma_{calc}(1 - \Delta)$$

The temperature dependence of Δ for the TG–$LiCF_3SO_3$ system shows that this parameter decreases with decreasing temperature and increasing concentration. Such behaviour agrees with the results found for $LiCF_3SO_3$ solutions in low-molecular-mass polyethylene glycol.[154, 155]

For the TG–$LiCF_3SO_3$ system, Δ increased from 0.81 to 0.88 in the temperature range of 40–80 °C (Fig. 24), which is attributable to a decrease in the free energy of ion pair formation with increasing temperature caused by the entropy effect. Such behaviour is in line with the results of Mössbauer spectroscopic examination of these electrolytes,[156] which demonstrated that the fraction of free ions decreases with temperature rise.

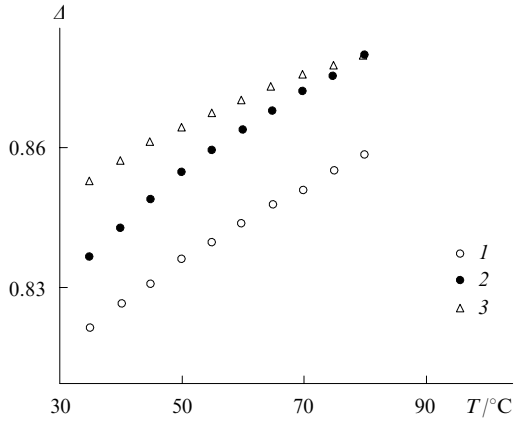


Figure 24. Temperature dependences of parameter Δ for the TG–$LiCF_3SO_3$ system with the O : Li ratio of 12 : 1 (*1*), 15 : 1 (*2*), 18 : 1 (*3*).[154]

For this system, the dependences of molar conductivity on the salt concentration demonstrated a narrow minimum in the low salt concentration region and a wide maximum at high salt concentrations.[157, 158] The pattern of this depend-

ence is not related to any irregularity in the viscosity and diffusion variations. Probably, the minimum is due to association of ions. For high salt concentrations, the number of ions increases as their concentration increases. The further insignificant decrease in the molar conductivity is associated with the sharp increase in solvent viscosity.

Gel-polymer electrolytes prepared by dissolving 30 mass % PVDF in the liquid electrolytes under consideration [154] were studied by NMR.[73, 160] The addition of the polymer induced a ~2-fold decrease in diffusion coefficients and conductivity, which was consistent with the results of other studies.[161, 162] Apparently, this is mainly due to the decrease in the ion transport velocity as a result of the increased tortuosity factor.

In PDVF–DMF–$LiCF_3SO_3$ gel electrolytes, the parameter Δ and, hence, the degree of ionic association increased with the increase in the salt concentration much more sharply than in solutions containing no polymers. In the PVDF–TG–$LiCF_3SO_3$ gel-electrolyte systems, the concentration dependence of Δ was similar to that in the original liquid electrolyte.[146, 156] However, in contrast to liquid systems, the parameter Δ in gel electrolytes based on DMF and TG decreased as the temperature rose. The weakening of ion association can be explained, on the one hand, by the transition of ions from the crystalline electrolyte domain to the 'liquid' domain, which leads to a higher number of mobile ions. One the other hand, the incorporation of neutral clusters and ion associates into the PVDF phase is possible. As a result, the relative fraction of dissociated ions in the liquid (mobile) electrolyte component increases.

The dependence of diffusion coefficients of ions and solvent on the $LiN(CF_3SO_2)_2$ salt content in gel-polymer electrolytes based on PVDF-HFP had the following characteristics:

— the lower the ion concentration, the higher the diffusion coefficients; this is explained by the fact that viscosity and the degree of salt dissociation depend on the solution concentration;

— diffusion coefficients decreased with the increase in the proportion of the polymer in the electrolyte;

— diffusion coefficients of cations and anions approached each other with the increase in the polymer content, which pointed to the joint transport of cations and anions at high polymer contents.

These features suggest that the degree of salt dissociation decreases with an increase in the proportion of the polymer component. Similar changes in the diffusion of ions were also observed for other salts.[164, 166, 167]

In polymers with a microporous structure, no dependence of diffusion coefficients of lithium ions on the diffusion time was noted in the range from 20 to 320 ms, which corresponds to the translational displacement of ions in the range from 2 to 10 μm. The diffusion decay curves contained two components with diffusion coefficients differing by an order of magnitude. After a certain period, only one diffusion coefficient was observed.[163, 168]

The polymer electrolyte based on 3D cross-linked polyester and $LiN(CF_3SO_2)_2$ salt was studied by DSC, impedance spectroscopy and NMR.[169] Lithium diffusion coefficients were much smaller than the diffusion coefficients of anions and independent of the diffusion time; at the same time, the diffusion coefficients of anions decreased with an increase in the diffusion time; this was more pronounced at low temperatures (Fig. 25). The presence of such dependence assumes the existence of restricted diffusion, which is of great interest for membrane studies. Unfortunately, the authors of the mentioned paper [169] did not discuss the nature of restrictions.

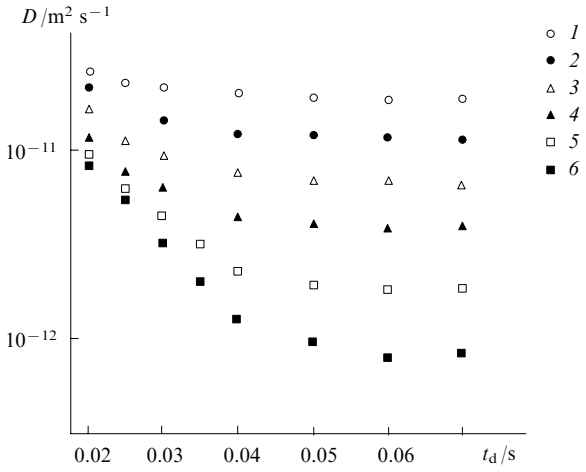


Figure 25. Diffusion coefficient of $N(CF_3SO_2)_2^-$ anions in a polyester-based polymer electrolyte *vs.* the diffusion time at temperatures 353 (1), 343 (2), 333 (3), 323 (4), 313 (5), 303 K (6).[169]

Lithium diffusion was studied in the system polyester diacrylate (PEDA)–lithium perchlorate–ethylene carbonate.[170] For a sample with a high EC content, the diffusion coefficient dependence had a step at ~30 °C (Fig. 26). Probably, such anomalous variation of the diffusion coefficient of lithium ions can be associated with the existence of an individual phase of lithium perchlorate solution in ethylene carbonate with the melting point equal to 36 °C. This assumption agrees with the fact that for samples with lower solvent concentrations, the temperature dependence of diffusion coefficients had no step and corresponded to the Arrhenius dependence. It deserves mention that the activation energy of diffusion is slightly higher than the activation energy of conduction.

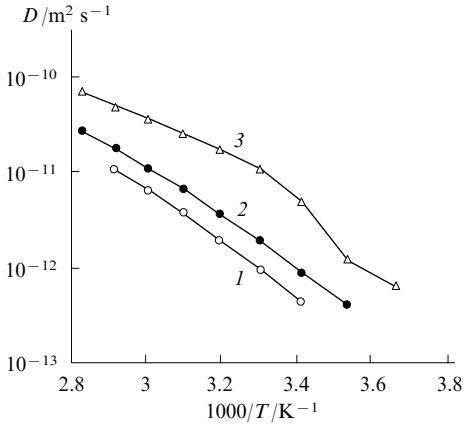


Figure 26. Temperature dependences of the diffusion coefficients of lithium ions in gel-polymer electrolytes based on PEDA with the EC content of 4.3 (*1*), 18.4 (*2*) and 54.8 mass % (*3*).[170]

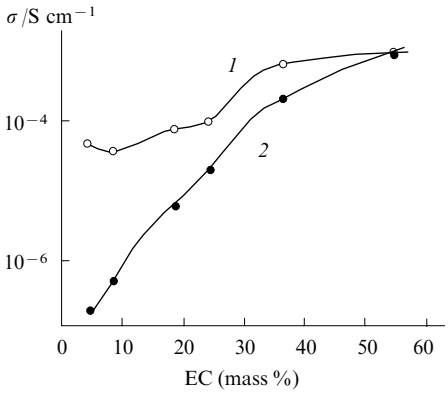


Figure 27. Ionic conductivity *vs*. the EC content in polymer electrolyte based on PEDA at temperature 30 °C.[170]
The specific conductivity was calculated according to the Nernst–Einstein equation (*1*) and measured by impedance spectroscopy (*2*).

In order to compare the data on lithium cation diffusion with experimental results on the ionic conductivity, the conductivity was calculated based on NMR spectroscopy data. Figure 27 shows the experimental and calculated dependences of conductivity on the ethylene carbonate content.

In the range of low solvent concentration, the calculated conductivity values exceeded the experimental conductivities by 1–2 orders of magnitude. As the solvent concentrations increased, the difference between these quantities became smaller and they virtually coincided at the maximum content of ethylene carbonate. The deviations of these dependences are attributable to the fact that the conductivity was calculated under the assumption that all lithium perchlorate molecules have dissociated and the number of lithium cations is equal to the number of lithium salt molecules in unit volume. Apparently, this can be true for large contents of ethylene carbonate but at its low contents, lithium perchlorate is not fully dissociated.

The translational mobility of solvent molecules in gel electrolytes based on polyester diacrylate and lithium perchlorate with different contents of solvent (ethylene carbonate) was studied by pulsed field gradient ^{1}H NMR method.[47] In addition to diacrylate units, the PEDA composition included hydroxyethyl acrylate and 1,6-dioxo-1,4-crown-4 (dimerization product of the initial monomer) units. For samples containing 12 mass % EC and higher, a triexponential diffusion decay was observed, whereas samples with the EC content below 12 mass % were characterized by biexponential decay. For instance, for a sample with 18.4 mass % EC (Fig. 28), the diffusion decay curve was well described by the sum of three exponents with diffusion coefficients of 3.3×10^{-13}, 2.7×10^{-12}, 2.7×10^{-11} m^2 s^{-1}, which corresponded to individual ethylene carbonate molecules (phase *I*), ethylene carbonate molecules solvating lithium cations (phase *II*) and crown-ether molecules (phase *III*). For the EC content of < 12 mass %, the slow component of diffusion decay was no longer observed. The spin echo signal was absent in polymers containing no EC. Probably, these factors were associated with the low mobility of crown ether molecules in PEDA with a low solvent content, which made negligible the apparent population of

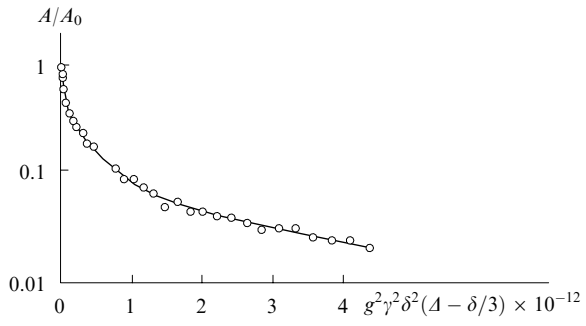


Figure 28. Diffusion decay of spin echo signals on ^{1}H nuclei for a gel-polymer electrolyte with the solvent content of 18.4 mass %.[47] Points correspond to experiment; curve is the least-square approximation by the sum of three exponents.

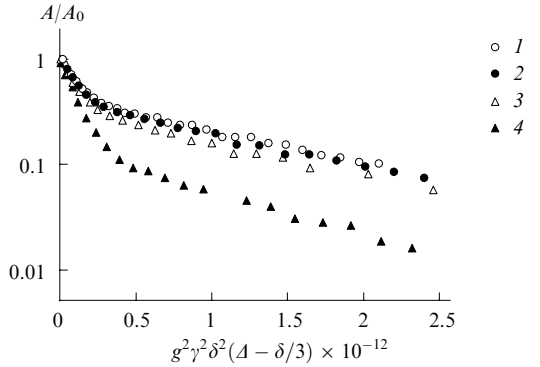


Figure 29. Diffusion decay of spin echo signals on ^{1}H nuclei for a sample containing 4.3% of the solvent for diffusion times of 10 (*1*), 20 (*2*), 35 (*3*), 120 ms (*4*).[47]

phase *III*. Figure 29 shows the diffusion decay curves in a sample containing 4.3 mass % EC plotted for different diffusion times. For small t_d values, the diffusion decay was independent of the diffusion time, which points to the slow molecular exchange between phases *I* and *II*. For longer diffusion times, the apparent population of phase *II* decreased with the increase in t_d, which is typical of the intermediate exchange between phases *I* and *II*. For a sample with the minimum content of solvent (4.3 mass %), the lifetime of EC molecules in phase *II* was 90 ms. The dependence of the phase population on the transverse relaxation time T_1 was neglected, because the relaxation times were not less than 600 ms, *i.e.*, they were longer than τ by an order of magnitude.

The diffusion coefficients of EC molecules in phase *II* depended insignificantly on the diffusion time. Thus, as the diffusion time changed from 20 to 600 ms, the diffusion coefficients were only halved. This also points to the relatively free exchange of solvent molecules between the phases.

The sufficiently fast exchange of solvent molecules between phases *I* and *II* also follows from the fact that the decay of longitudinal magnetization was characterized by a single spin–lattice relaxation time, which varied from 600 ms to 1 s and depended on the content of the solvent.

5. Electrophoretic pulsed field gradient NMR method

The pulsed field gradient NMR method makes it possible to selectively measure the diffusion coefficients of ions.[173] A modification of this method (application of an electric field to the sample under study) is suitable for non-destructive measurements of ion mobilities. The charged particles can be metal cations, *e.g.*, Li^+, Na^+, Cs^+, or multiatomic ions such as alkylammonium or polyelectrolyte ions and also charged molecular aggregates such as micelles. The classical electrochemical methods provide integral mobilities and transfer numbers for all charge carriers. Of special interest are the studies of mobility of individual ions in porous media and polymer electrolytes.

Holz and Muller[174] carried out the first experimental study of the drift velocity of Et_4N^+ ions in water in the external electric field. They combined electrophoresis and the selective NMR spectroscopy.§

Under the effect of electric field, ions acquire a constant velocity

$$v_\pm = \mu_\pm E$$

where $\mu_\pm$ is the ion mobility.

Theoretical calculations of mobility $\mu_\pm$ are very complicated[177] and it is determined experimentally. For strong electrolytes, from known $v_\pm$, one can obtain another very important parameter, the transfer number. The procedures of calculation of these values were described in detail.[174, 176]

When performing such an experiment, it is important that the electric field intensity in the electrolyte be maintained constant. In two-electrode cells[178] where the same electrodes are used as both the blocking and the indicator electrodes, the electric potential at the electrode/electrolyte interface decreases due to electrolyte polarization[179] and also due to chemical changes that take place in near-electrode electrolyte.[180] As a result of these factors, the electric field intensity in the electrolyte bulk changes. To solve this problem, a four-electrode cell (Fig. 30) was used, which made it possible to maintain a constant electric field intensity throughout the sample bulk between the indicator electrodes.

The gel-polymer electrolyte 1 M $LiN(CF_3SO_2)_2$–EC/DEC–PVDF-HFP was studied by electrophoretic NMR in a four-electrode cell.[181] Figure 31 shows the dependences of velocity of motion of various nuclei on the applied voltage. For voltage of 512 V, the ion velocity varied linearly with the voltage and no motion was observed for solvent molecules. The mobilities of Li^+ and $N(CF_3SO_2)_2^+$ ions were found to be 7.2×10^{-5} and 1.4×10^{-4} cm^2 s^{-1} V^{-1}, respectively. Based on the data on the conductivity and the diffusion coefficients of lithium ions (1.5×10^{-6} cm^2 s^{-1}) and fluoride ions (1.9×10^{-6} cm^2 s^{-1}), the transfer numbers were found to be 0.34 and 0.44, respectively.

The deviations between the transfer numbers found by different methods may be due to the contribution of ion pairs to the diffusion coefficients measured by the NMR method.

§ The name 'electrophoretic NMR' (ENMR) appeared for the first time in Ref. 175. The term 'electrophoretic' is used to designate translational motion of all types of charges in the electric field. Generally, for all direct-current NMR experiments, the abbreviation DCNMR is used.[176]

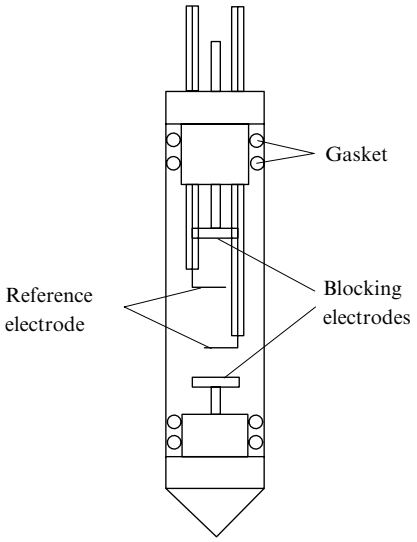


Figure 30. Illustration of a four-electrode cell for electrophoretic NMR.[181]

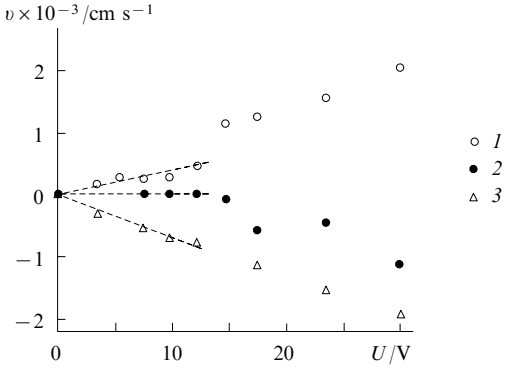


Figure 31. Motion velocities of various nuclei *vs.* the reference electrode potential (U) in the $LiN(CF_3SO_2)_2$–EC/DEC–PVDF-HFP system.[181]
(*1*) ^{7}Li, (*2*) ^{1}H, (*3*) ^{19}F.

Hayamizu *et al.*[182] studied the lithium transport in $LiN(CF_3SO_2)_2$–PC electrolytes by the electrophoretic NMR method in a two-electrode cell with lithium electrodes. The maximum voltage used in these experiments was 3 V, which is below the decomposition voltage for electrolytes under study. The application of an electric field had insignificant effect on the self-diffusion coefficients of the solvent and the ions.

VII. Conclusion

Nowadays, chemical power sources, particularly, lithium batteries and fuel cells find wide application. The principal part of these systems is formed by a polymer electrolyte that should have high ionic conductivity. The problem of finding the mechanism of ion transport in these polyelectrolytes becomes quite challenging. The last decade was characterized by active studies of the state and mobility of cations and molecules in lithium-conducting polymers and ion-exchange membranes of various types by using the methods

of NMR and pulsed field gradient NMR on various nuclei. Despite the numerous publications, no reviews on this subject are known.

The authors of the present review tried to fill this gap.

The possibilities of investigating the mechanisms of ion and molecular transport in ion-exchange membranes by elucidating the relationship between the nanostructure of the polymer matrix and the microscopic state and mobilities of ions and molecules determined by the NMR methods were discussed. Attention was focused on the peculiarities of ion transfer under the conditions of low moisture content.

This problem is challenging because its solution can advance the development of theoretical concepts on the electro and mass transfer in membranes, the targeted synthesis of highly selective membranes of new generation and the optimization of membrane separation processes.

The results of the research into the polymer structure and ionic mobility in polymer electrolytes for lithium cells were generalized. It was shown that the today NMR techniques such as high-resolution NMR spectroscopy in solids, NMR relaxation, pulsed field gradient NMR and electrophoretic NMR make it possible to acquire unique information on the structural and dynamic characteristics of these systems.

This study was carried out with financial support from the Russian Foundation of Basic Research (Project No. 10-03-00862-a).

References

1. S T Hwang, K Kammermeyer *Membranes in Separations* (New York: Wiley Interscience, 1975)
2. A E Chalykh *Diffuziya v Polimernykh Sistemakh* (Diffusion in Polymer Systems) (Moscow: Khimiya, 1987)
3. V A Shaposhnik *Kinetika Elektrodializa* (Kinetics of Electrodialysis) (Voronezh: Voronezh State University, 1989)
4. N I Nikolaev *Diffuziya v Membranakh* (Diffusion in Membranes) (Moscow: Khimiya, 1980)
5. S F Timashev *Fizikokhimiya Membrannykh Protsessov* (Physical Chemistry of Membrane Processes) (Moscow: Khimiya, 1988)
6. A B Yaroslavtsev *Khimiya Tverdogo Tela* (The Chemistry of Solid) (Moscow: Nauchnyi Mir, 2009)
7. V I Zabolotskii, V V Nikonenko *Perenos Ionov v Membranakh* (Ion Transfer in Membranes) (Moscow: Nauka, 1996)
8. G P Vishnevskaya, L S Molochnikov, R Sh Safin *EPR v Ionitakh* (ESR in Ionites) (Moscow: Nauka, 1992)
9. R Vázquez, J Ávalos, F Volino, M Pineri, D Galland *J. Appl. Polym. Sci.* **28** 1093 (1983)
10. S Schlick, M G Alonso-Amigo *Macromolecules* **22** 2634 (1989)
11. V I Volkov, S N Gladkikh, S F Timashev, N I Smirnov, V I Muromtsev, A I Andreeva, S V Timofeev *Khim. Fiz.* **13** (1) 49 (1993) [a]
12. V I Volkov, S F Timashev *Zh. Fiz. Khim.* **63** 209 (1989) [b]
13. G Martini, M F Ottaviani, L Pedocchi, S Ristovi *Macromolecules* **22** 1743 (1989)
14. L Kevan, L D Kispert *Electron Spin Double Resonance Spectroscopy*. Wiley New York 1976
15. V I Volkov, V I Muromtsev, K K Pukhov, S F Timashev, G A Balaev *Dokl. Akad. Nauk SSSR* **276** 395 (1984) [c]
16. V I Volkov, V I Muromtsev, K K Pukhov, G A Grigor'eva, N I Nikolaev *Dokl. Akad. Nauk SSSR* **239** 1125 (1978) [c]
17. V I Volkov, K K Pukhov, S H Choh, I-W Park, E V Volkov *Appl. Magn. Res.* **24** 177 (2003)
18. A N Ozerin, A V Rebrov, A N Yakunin, L P Bogovtseva, S F Timashev, N F Bakeev *Vysokomol. Soedin., Ser. A* **28** 254 (1986) [d]
19. A N Ozerin, A V Rebrov, A N Yakunin, N P Bessonova, N A Dreiman, L F Sokolov, N F Bakeev *Vysokomol. Soedin., Ser. A* **28** 2303 (1986) [d]
20. A E King *Ion Containing Polymers. Physical Properties and Structure* (New York: Academic Press, 1977)
21. M Fujimura, T Hashimoto, H Kawai *Macromolecules* **14** 1309 (1981)
22. M Fujimura, T Hashimoto, H Kawai *Macromolecules* **15** 136 (1982)
23. G S Bystrov, G A Grigor'eva, N I Nikolaev *Russ. Chem. Rev.* **45** 823 (1976)
24. V V Mank, O D Kurilenko *Issledovanie Mezhmolekulyarnykh Vzaimodeistvii v Ionoobmennykh Smolakh Metodom YaMR* (Investigation of Intermolecular Interactions in Ion-Exchange Resins by NMR) (Kiev: Naukova Dumka, 1976)
25. V V Mank, N I Lebovka *Voda v Dispersnykh Sistemakh* (Water in Dispersion Systems) (Moscow: Khimiya, 1989)
26. G K Saldadze, R I Tagirova, V I Volkov, S A Chizhanov *Zh. Fiz. Khim.* **67** 1818 (1993) [b]
27. V I Volkov, G K Saldadze, R I Tagirova, L V Kropotov, V G Khutsishvili, N N Shapet'ko *Zh. Fiz. Khim.* **63** 1005 (1989) [b]
28. V G Khutsishvili, Yu S Bogachev, V I Volkov, B V Tarasova, N A Dreiman, N N Shapet'ko, S F Timashev *Zh. Fiz. Khim.* **58** 2633 (1984) [b]
29. V I Volkov, E A Sidorenkova, S F Timashev, S G Lakeev *Zh. Fiz. Khim.* **67** 1014 (1993) [b]
30. V I Volkov, A A Pavlov, E A Sanginov *Solid State Ionics* **188** 124 (2010)
31. V I Volkov, E V Volkov, S V Timofeev, E A Sanginov, A A Pavlov, E Yu Safronova, I A Stenina, A B Yaroslavtsev *Zh. Neorg. Khim.* **55** 358 (2010) [e]
32. N J Bunce, S J Sondheimer, C A Fyfe *Macromolecules* **19** 333 (1986)
33. G Ye, N Janzen, G R Goward *Macromolecules* **39** 3283 (2006)
34. S L Shestakov, A A Pavlov, A V Maksimychev, A V Chernyak, V I Volkov, S V Timofeev *Khim. Fiz.* **29** (12) 60 (2010) [a]
35. R A Komoroski, K A Mauritz *J. Am. Chem. Soc.* **100** 7487 (1978)
36. R A Komoroski *Adv. Chem.* **187** 155 (1980)
37. V I Volkov, E A Sidorenkova, S A Korochkova, N A Novikov, I B Sokol'skaya, S F Timashev *Zh. Fiz. Khim.* **68** 309 (1994) [b]
38. V I Volkov, E A Sidorenkova, S A Korochkova, N A Novikov, I B Sokol'skaya, S F Timashev *Zh. Fiz. Khim.* **68** 559 (1994) [b]
39. D A Lysak, A A Marinin, A F Shestakov, V I Volkov, in *Nuclear Magnetic Resonance in Condensed Matter* (St Petersburg: St Petersburg State University, 2011) p. 120
40. V Volkov, A Marinin, in *Nuclear Magnetic Resonance in Condensed Matter* (St Petersburg: St Petersburg State University, 2011) p.221
41. P Kuo, W Liang, T Chen *Polymer* **44** 2957 (2003)
42. J A Chaker, K Dahmouche, C V Santilli, S H Pulcinelli, V Briois, A-M Frank, P Judeinstein *J. Non-Cryst. Solids* **304** 109 (2002)
43. H-M Kao, P-C Chang, S-W Chao, C-H Lee *Electrochim. Acta* **52** 1015 (2006)
44. D Saikia, Y W Chen-Yang, Y T Chen, Y K Li, S I Lin *Electrochim. Acta* **54** 1218 (2009)

45. P Mustarelli, E Quartarone, C Capiglia, C Tomasi, P Ferloni, A Magistris *J. Chem. Phys.* **111** 3761 (1999)
46. S Licoccia, M Trombetta, D Capitani, N Proietti, P Romagnoli, M L Di Vona *Polymer* **46** 4670 (2005)
47. A A Marinin, K G Khatmullina, V I Volkov, O V Yarmolenko, V A Zabrodin *Russ. Chem. Bull. (Int. Ed.)* **60** 1096 (2011)
48. J J Dechter *J. Polym. Sci., Polym. Lett. Ed.* **23** 261 (1985)
49. T K-J Klster, L van Wmllen *Solid State Ionics* **178** 1879 (2008)
50. T Gullion, J Schaefer, in *Advances in Magnetic Resonance* Vol. 13 (New York: Academic Press, 1989) p. 57
51. Y G Andreev, P Lightfoot, P G Bruce *Chem. Commun.* 2169 (1996)
52. K Thieme, I Schnell *J. Am. Chem. Soc.* **125** 12100 (2003)
53. W J Blaedel, L E Brower, T L James, J H Noggle *Anal. Chem.* **44** 982 (1972)
54. N G Boyle, V J McBrierty, D C Douglass *Macromolecules* **16** 75 (1983)
55. V I Volkov, I A Nesterov, A V Chichagov, V I Muromtsev, S F Timashev *Khim. Fiz.* **4** (5) 644 (1985) [a]
56. V I Volkov, I A Nesterov, S F Timashev, V I Sundukov, L V Kropotov *Khim. Fiz.* **8** (1) 128 (1989) [a]
57. V I Volkov, S L Vasilyak, I-W Park, H J Kim, H Ju, E V Volkov, S H Choh *Appl. Magn. Res.* **25** 43 (2003)
58. V I Volkov, E V Volkov, S F Timashev, in *Magnetic Resonanse in Colloid and Interface Science* (Dordrecht: Kluwer Academic, 2002) p. 267
59. V I Volkov, E V Volkov, S L Vasilyak, Y S Hong, C H Lee, in *Fluid Transport in Nanoporous Materials* (New York: Springer, 2006) p. 48
60. M Goldsmith, D Hor, R Damadian *J. Chem. Phys.* **65** 1708 (1976)
61. M Levij, J De Bleijser, J C Leyte *Chem. Phys. Lett.* **83** (1) 183 (1981)
62. C J M Van Rijn, A J Maat, J de Bleijser, J C Leyte *Chem. Phys. Lett.* **135** (1 2) 57 (1987)
63. C J M Van Rijn, A J Maat, J de Bleijser, J C Leyte *J. Phys. Chem.* **93** 5284 (1989)
64. R H Tromp, J R C van der Maarel, J de Bleijser, J C Leyte *Biophys. Chem.* **41** 81 (1991)
65. I A Nesterov, V I Volkov, K K Pukhov, S F Timashev *Khim. Fiz.* **10** (8) 1155 (1990) [a]
66. V I Volkov, Yu G Eliseev, Yu E Kirsh, Yu A Fedotov, S F Timashev *Zh. Fiz. Khim.* **66** 1618 (1992) [b]
67. C E Tambelli, J P Donoso, C J Magon, E C Pereira, A V Rosario *Electrochim. Acta* **53** 1535 (2007)
68. D P Tunstall, A S Tomkin, J R MacCallum, C A Vincent *J. Phys. C* **21** 1039 (1988)
69. M Forsyth, M Garcia, D R MacFarlane, S Ng, M E Smith, J H Strange *Solid State Ionics* **86–88** 1365 (1996)
70. F Ali, M Forsyth, M C Garcia, M E Smith, J H Strange *Solid State Nucl. Magn. Res.* **5** 217 (1995)
71. M Forsyth, D R MacFarlane, P Meakin, M E Smith, T J Bastow *Electrochim. Acta* **40** 2343 (1995)
72. S Suarez, J Jayakody, S Abbrent, S G Greenbaum, J H Shin, S Passerini *Solid State Ionics* **176** 1113 (2005)
73. M J Williamson, H V St A Hubbard, I M Ward *Polymer* **40** 7177 (1999)
74. E O Stejkal, J E Tanner *J. Chem. Phys.* **42** 288 (1965)
75. A I Maklakov, V D Skirda, N F Fatkulin *Samodiffuziya v Rastvorakh i Rasplavakh Polimerov* (Self-diffusion in Solutions and Melts of Polymers) (Kazan: Kazan State University, 1987)
76. G K Saldadze, R I Tagirova, V I Volkov, S A Chizhanov *Zh. Fiz. Khim.* **67** 1941 (1993) [b]
77. G K Saldadze, V I Volkov, R I Tagirova, S A Chizhanov *Zh. Fiz. Khim.* **67** 773 (1993) [b]
78. V I Volkov, S A Korochkova, I A Nesterov, Yu E Kirsh, S F Timashev *Zh. Fiz. Khim.* **68** 1310 (1994) [b]
79. V I Volkov, S A Korochkova, S F Timashev *Zh. Fiz. Khim.* **69** 1124 (1995) [b]
80. V I Volkov, S A Korotchkova, H Ohya, Q Guo *J. Membr. Sci.* **100** 273 (1995)
81. S A Sokolova, O V Djakonova, V V Kotov, Y S Hong, V I Volkov, C H Lee *Magn. Res. Imag.* 19 (2001)
82. V I Volkov, S A Korotchkova, I A Nesterov, H Ohya, Q Guo, J Huang, J Chen *J. Membr. Sci.* **110** 1 (1996)
83. E N Vasina, V D Skirda, V I Volkov, A N Nechaev, B V Mchedlishvili *Zh. Fiz. Khim.* **73** 285 (1999) [b]
84. V I Volkov, Yu M Popkov, S F Timashev, D G Bessarabov, R D Sanderson, Z Twardowski *J. Membr. Sci.* **180** 1 (2000)
85. V VKotov, O V D'yakonova, S A Sokolova, V I Volkov *Elektrokhimiya* **38** 994 (2002) [f]
86. V I Volkov, V V Kotov, G A Netesova *Zh. Fiz. Khim.* **82** 1337 (2008) [b]
87. A N Ponomarev, Yu A Dobrovol'skii, E F Abdrashitov, V Ch Bokun, E A Sanginov, E V Volkov, V I Volkov *Izv. Akad. Nauk, Energetika* (3) 124 (2008)
88. V I Volkov, Yu A Dobrovolsky, M S Nurmiev, E A Sanginov, E V Volkov, A V Pisareva *Solid State Ionics* **179** 148 (2008)
89. V I Volkov, A N Ponomarev, A B Yaroslavtsev, E A Sanginov, A A Pavlov *Al'ternat. Energ. Ekol.* (2) 99 (2008) [g]
90. E Yu Voropaeva, E A Sanginov, V I Volkov, A A Pavlov, A S Shalimov, I A Stenina, A B Yaroslavtsev *Zh. Neorg. Khim.* **53** 1643 (2008) [e]
91. C L Shestakov, A A Pavlov, A V Maksimychev, A V Chernyak, V I Volkov, S V Timofeev *Khim. Fiz.* **29** (12) 60 (2010) [a]
92. V I Volkov, A A Pavlov, Yu A Fedotov, A A Marinin *Zh. Fiz. Khim.* **84** 1868 (2010) [b]
93. V I Volkov, E V Volkov, S V Timofeev, E A Sanginov, A A Pavlov, E Yu Safronova, I A Stenina, A B Yaroslavtsev *Zh. Neorg. Khim.* **55** 355 (2010) [e]
94. E Y Safronova, V I Volkov, A B Yaroslavtsev *Solid State Ionics* **188** 129 (2011)
95. V I Volkov, E V Volkov *Appl. Magn. Res.* **29** 495 (2005)
96. S Tsushima, K Teranishi, S Hirai *Energy* **30** 235 (2005)
97. V Baglio, A S Aricò, V Antonucci, I Nicotera, C Oliviero, L Coppola, P L Antonucci *J. Power Sources* **163** 52 (2006)
98. C A Edmondson, P E Stallworth, M E Chapman, J J Fontanella, M C Wintersgill, S H Chung , S G Greenbaum *Solid State Ionics* **135** 419 (2000)
99. H A Every , M A Hickner, J E McGrath, T A Zawodzinski Jr *J. Membr. Sci.* **250** 183 (2005)
100. J R P Jayakody, A Khalfan, E S Mananga, S G Greenbaum, T D Dang, R Mantz *J. Power Sources* **156** 195 (2006)
101. V Freger, E Korin, J Wisniak, E Korngold, M Ise, K D Kreuer *J. Membr. Sci.* **160** 213 (1999)
102. X Gong, A Bandis, A Tao, G Meresi, Y Wang, P T Inglefield, A A Jones, W-Y Wen *Polymer* **42** 6485 (2001)
103. A N Khalfan, L M Sanchez, Ch Kodiweera, S G Greenbaum, Z Bai, T D Dang *J. Power Sources* **173** 853 (2007)
104. Y F Huang, L C Chuang, A M Kannan, C W Lin *J. Power Sources* **186** 22 (2009)
105. F Hallberg, T Vernersson, E T Pettersson, S V Dvinskikh, G Lindbergh, I Furó *Electrochim. Acta* **55** 3542 (2010)
106. D A Kritskaya, E F Abdrashidov, V Ch Bokun, A I Ponomarev, A V Chernyak, S G Vasil'ev, V I Volkov *Memb. Membr. Tekhnol.* **1** 266 (2011) [h]
107. T D Gierke, G E Munn, F C Wilson *J. Polym. Sci., Polym. Phys. Ed.* **19** 1687 (1981)
108. W Y Hsu, T D Gierke *J. Membr. Sci.* **13** 307 (1983)
109. K A Mauritz, R B Moore *Chem. Rev.* **104** 4535 (2004)

110. D A Mologin, P G Khalatur, A R Khokhlov *Macromol. Theor. Simul.* **11** 587 (2002)
111. F Kh Chibirova, D S Zakhar'in, V E Sedov, S F Timashev, Yu M Popkov, S I Reiman *Khim. Fiz.* **6** (8) 1137 (1987) [a]
112. Yu M Vol'fkovich, V K Luzhin, A N Vanyulin, E I Shkol'nikov, I A Blinov *Elektrokhimiya* **20** 656 (1984) [f]
113. Yu E Kirsh, Yu F Fedotov, I A Iudina, D Yu Artemov, N A Yanul', T N Nekrasova *Vysokomol. Soedin., Ser. A* **33** 1127 (1991) [d]
114. Yu E Kirsh, I M Malkina, Yu A Fedotov, N A Yanul', S S Gittis, S A Smirnov, S F Timashev *Vysokomol. Soedin., Ser. A* **35** 320 (1993) [d]
115. A L Rusanov, E G Bulycheva, M G Bugaenko, V Yu Voytekunas, M J Abadie *Russ. Chem. Rev.* **78** 53 (2009)
116. Yu A Dobrovol'skii, A V Pisareva, L S Leonova, A I Karelin *Al'ternat. Energ. Ekol.* (12) 36 (2004) [g]
117. V I Volkov, A I Rebrov, E A Sanginov, E M Anokhin, S L Shestakov, A A Pavlov, A V Maksimychev, Yu A Dobrovol'skii *Elektrokhimiya* **45** 398 (2009) [f]
118. A Kedrinskii, V E Dmitrenko, I I Grudyanov, in *Litievye Istochniki* (Litium Sources) (Moscow: Energoatomizdat, 1992) p. 241
119. V S Bagotskii, A M Skundin *Khimicheskie Istochniki Toka* (Chemical Current Sources) (Moscow: Energoizdat, 1981)
120. A A Taganova, I A Pak *Germetichnye Khimicheskie Istochniki Toka dlya Portativnoi Apparatury. Spravochnik* (Sealed Chemical Current Sources for Portable Equipment) (Moscow: Khimizdat, 2003)
121. A L L'vov *Soros. Obrazovat. Zh.* **7** (3) 45 (2001) [i]
122. V S Bagotskii, A M Skundin *Elektrokhimiya* **31** 342 (1995) [f]
123. A M Skundin, O N Elfimov, O V Yarmolenko *Russ. Chem. Rev.* **71** 329 (2002)
124. O V Yarmolenko, K G Khatmullina *Al'ternat. Energ. Ekol.* (3) 59 (2010) [g]
125. A M Stephan, K S Nahm *Polymer* **47** 5952 (2006)
126. A M Stephan *Eur. Polym. J.* **42** 21 (2006)
127. V Chandrasekhar *Polymer Solid Electrolytes: Synthesis and Structure* (New York: Springer, 1996)
128. W Wieczorek *Mater. Sci. Eng. B* **15** 108 (1992)
129. W Gang, J Roos, D Brinkmann, F Capuano, F Croce, B Scrosati *Solid State Ionics* **53 – 56** 1102 (1993)
130. F Croce, R Curini, A Martinelli, L Persi, F Ronci, B Scrosati *J. Phys. Chem.* **103** 10632 (1999)
131. B Kumar, L G Scanlon *Solid State Ionics* **124** 239 (1999)
132. E A Ukshe, N G Bukun *Tverdye Elektrolity* (Solid Electrolytes) (Moscow: Nauka, 1977)
133. N G Bukun, A E Ukshe, E A Ukshe *Elektrokhimiya* **29** 110 (1993) [f]
134. T E Gough, H D Sharma, N Subramanian *Can. J. Chem.* **48** 917 (1970)
135. H D Sharma, N Subramanian *Can. J. Chem.* **49** 457 (1971)
136. R W Creekmore, Ch N Reilley *Anal. Chem.* **42** 570 (1970)
137. D Massiot, F Fayon, M Capron, I King, S Le Calvé, B Alonso, J-O Durand, B Bujoli, Z Gan, G Hoatson *Magn. Res. Chem.* **40** 70 (2002)
138. D Reichert,O Pascui, P Judeinstein, T Gullion *Chem. Phys. Lett.* **402** 43 (2005)
139. Z Gadjourova, D M Marero, K H Andersen, Y G Andreev, P G Bruce *Chem. Mater.* **13** 1282 (2001)
140. US P. 3330697 (1967)
141. W Huang, R Frech, P Johansson, J Lindgren *Electrochim. Acta* **40** 2147 (1995)
142. S Bhattacharja, S W Smoot, D H Whitmore *Solid State Ionics* **18 – 19** 306 (1986)
143. P G Bruce, C A Vincent *J. Chem. Soc., Faraday Trans.* **89** 3187 (1993)
144. S H Chung, K R Jeffrey, J R Stevens *J. Chem. Phys.* **94** 1803 (1991)
145. M J Williamson, J P Southall, H V St A Hubbard, S F Johnston, G R Davies, I M Ward *Electrochim. Acta* **43** 1415 (1998)
146. M J Williamson, J P Southall, H V St A Hubbard, G R Davies, I M Ward *Polymer* **40** 3945 (1999)
147. K Hayamizu, Y Aihara *Electrochim. Acta* **49** 3397 (2004)
148. Y Matsuda, M Morita, F Tachihara *Bull. Chem. Soc. Jpn.* **59** 1967 (1986)
149. M S Ding, T R Jow *J. Electrochem. Soc.* **150** A620 (2003)
150. M S Ding *J. Chem. Eng. Data* **48** 519 (2003)
151. K Hayamizu, Y Aihara, S Arai, C G Martinez *J. Phys. Chem. B* **103** 519 (1999)
152. Y Aihara, K Sugimoto, W S Price, K Hayamizu *J. Chem. Phys.* **113** 1981 (2000)
153. Y Aihara, T Bando, H Nakagawa, H Yoshida, K Hayamizu, E Akiba, W S Price *J. Electrochem. Soc.* **151** A119 (2004)
154. M J Williamson, J P Southall, H V St A Hubbard, S F Johnston, G R Davies, I M Ward *Electochim. Acta* **43** 1415 (1998)
155. N Boden, S A Leng, I V Ward *Solid State Ionics* **45** 261 (1991)
156. I M Ward, N Boden, J Cruickshank, S A Ling *Electrochim. Acta* **40** 2071 (1995)
157. S F Johnston, I M Ward, J M Cruickshank, G R Davies *Solid State Ionics* **90** 39 (1996)
158. P G Hall, G R Davies, I M Ward, J E McIntyre *Polym. Commun.* **27** 100 (1986)
159. J R MacCallum, A S Tomlin, C A Vincent *Eur. Polym. J.* **22** 787 (1986)
160. I M Ward, M J Williamson, H V St A Hubbard, J P Southall, G R Davies *J. Power Sources* **81 – 82** 700 (1999)
161. J P Southall, H V St A Hubbard, S F Johnston, V Rogers, G R Davies, J E McIntyre, I M Ward *Solid State Ionics* **85** 51 (1996)
162. JP Southall, Ph.D. Thesis, University of Leeds, Leeds, 1995
163. Y Saito, H Kataoka, T Sakai, Sh Deki *Electrochim. Acta* **46** 1747 (2001)
164. C Capiglia, Y Saito, H Yamamoto, H Kageyama, P Mustarelli *Electrochim. Acta* **45** 1341 (2000)
165. H Kataoka, Y Saito, T Sakai, E Quartarone, P Mustarelli *J. Phys. Chem. B* **104** 11460 (2000)
166. Y Saito, H Kataoka, C Capiglia, H Yamamoto *J. Phys. Chem. B* **104** 2189 (2000)
167. Y Saito, C Capiglia, H Kataoka, H Yamamoto, H Ishikawa, P Mustarelli *Solid State Ionics* **136 – 137** 1161 (2000)
168. Y Saito, A M Stephan, H Kataoka *Solid State Ionics* **160** 149 (2003)
169. Y Aihara, K Hayamizu, K Sugimoto, T Bando, T Iguchi, J Kuratomi, T Ono, K Kuwana *J. Power Sources* **97 – 98** 628 (2001)
170. A A Marinin, K G Khatmullina, V I Volkov, O V Yarmolenko *Elektrokhimiya* **47** 766 (2011) [f]
171. K J Suh, Y S Hong, V D Skirda, V I Volkov, C-Y J Lee, C-H Lee *Biophys. Chem.* **104** 121 (2003)
172. J H Cho, Y S Hong, V D Skirda, V I Volkov *Magn. Res. Imag.* **21**1009 (2003)
173. Y A Every, M A Hichner, G E McGrath, T A Zavodzinskj *J. Membr. Sci.* **250** 183 (2006)
174. M Holz, C Muller *Ber. Bunsen-Gas. Phys. Chem.* **86** 141 (1982)
175. C S Johnson Jr, Q He *Adv. Magn. Res.* **13** 131 (1989)
176. M Holz *Chem. Soc. Rev.* **23** 165 (1994)
177. P Turq, J Barthel, M Chemla *Transport, Relaxation and Kinetic Processes in Electrolyte Solutions* (Berlin, Heidelberg, New York: Springer, 1992)
178. K M Abraham, in *Application of Electroactive Polymers* (London: Chapman and Hall, 1993) p. 175
179. Y Saito, H Kataoka, C Capiglia, H Yamamoto *J. Chem. Phys., B* **104** 2189 (2000)

180. M Y Qureshi, D Berstan, G G Cameron, M P Ingram, C Rousselot *Polym. Int.* **47** 16 (1998)
181. H Kataoka, Y Saito , Y Miyazaki, S Deki *Solid State Ionics* **152–153** 175 (2002)
182. K Hayamizu, S Seki, H Miyashiro, Y Kobayashi *J. Phys. Chem. B* **110** 22302 (2006)

[a] — *Russ. J. Phys. Chem., Ser. B (Engl. Transl.)*
[b] — *Russ. J. Phys. Chem., Ser. A (Engl. Transl.)*
[c] — *Dokl. Phys. Chem. (Engl. Transl.)*
[d] — *Polym. Sci. (Engl. Transl.)*
[e] — *Russ. J. Inorg. Chem. (Engl. Transl.)*
[f] — *Russ. J. Electrochem. (Engl. Transl.)*
[g] — *Int. Sci. J. Altern. Energ. Ecol. (Engl. Transl.)*
[h] — *Membr. Membr. Technol. (Engl. Transl.)*
[i] — *Soros Educ. J. (Engl. Transl.)*